Minnesota Department of Transportation

RESEARCH SERVICES & LIBRARY

Office of Transportation System Management

Automatic Generation of Traffic Signal Timing Plan

Henry X. Liu, Principal Investigator
Department of Civil, Environmental, and Geo- Engineering
University of Minnesota

September 2014

Research Project
Final Report 2014-38

To request this document in an alternative format call 651-366-4718 or 1-800-657-3774 (Greater Minnesota) or email your request to ADArequest.dot@state.mn.us. Please request at least one week in advance.

Technical Report Documentation Page

1. Report No.	2.	3. Recipients Accession No.	
MN/RC 2014-38			
4. Title and Subtitle Automatic Generation of Traffic Signal Timing Plan		5. Report Date September 2014	
		6.	
7. Author(s) Henry X. Liu and Jianfeng Zheng		8. Performing Organization Report No.	
9. Performing Organization Name and Address Department of Civil, Environmental, and Geo- Engineering University of Minnesota 500 Pillsbury Dr. S.E. Minneapolis, Minnesota 55455-0220		10. Project/Task/Work Unit No. CTS Project # 2013041	
		11. Contract (C) or Grant (G) No. (c) 99008 (wo) 67	
12. Sponsoring Organization Name and Address Minnesota Department of Transportation Research Services & Library 395 John Ireland Boulevard, MS 330 St. Paul, MN 55155		13. Type of Report and Period Covered Final Report	
		14. Sponsoring Agency Code	
15. Supplementary Notes http://www.lrrb.org/pdf/201438.pdf			

16. Abstract (Limit: 250 words)

Due to budget constraints, most of the traffic signals in the US are retimed once every 2-5 years. Despite that, traffic delay increases 3-5% per year with outdated timing plans. It would be desirable to reduce the signal retiming costs by automating all or a portion of the manual process. This research takes one step forward in this direction. In this project, we develop a performance visualization and fine-tuning tool for arterial traffic signal systems, aimed at reducing the labor costs for signal retiming. Using high-resolution event-based data from the SMART-Signal system, a set of easy-to-use algorithms are developed to refine traffic signal systems. Specifically, a framework is developed to diagnose operational problems regarding cycle lengths, green splits and offsets. Then, algorithms for offsets and green splits fine-tuning are proposed. To fine-tune offsets, a practical procedure to construct time space diagram (TS-Diagram) to visualize the progression quality on arterials is proposed and validated. For green splits, an adjusted measure of effectiveness (MOE), the utilized green time (UGT), is proposed for performance evaluation. Moreover, a practical procedure for time of day (TOD) transitions is also developed to generate optimal timing plan schedules. Field case studies and simulation experiments are carried out to illustrate and validate the proposed algorithms. The algorithms could be used during the retiming process to help agencies reduce labor costs, or to periodically refine traffic signal systems for coordinated arterials.

17. Document Analysis/Descriptors	18. Availability Statement		
Traffic signal control systems, Traffic signal timing, Algorithms, SMART-SIGNAL System, Labor costs	No restrictions. Document available from: National Technical Information Services, Alexandria, Virginia 22312		
19. Security Class (this report) Unclassified	20. Security Class (this page) Unclassified	21. No. of Pages 67	22. Price

Automatic Generation of Traffic Signal Timing Plan

Final Report

Prepared by:

Henry X. Liu
Jianfeng Zheng
Department of Civil, Environmental, and Geo- Engineering
University of Minnesota

September 2014

Published by:

Minnesota Department of Transportation
Research Services & Library
395 John Ireland Boulevard, MS 330
St. Paul, Minnesota 55155-1899

Acknowledgments

This work was supported by Minnesota Department of Transportation. The authors would like to thank Steve Misgen, Timothy Bangsund, and Curt Krohn from MnDOT for their assistance in the field deployment of the SMART-Signal system. Kevin Schwartz and Nicole Flint from MnDOT also offered constructive advices for this research. Their assistance is acknowledged.

Dr. Henry Liu and the University of Minnesota have equity and royalty interests in SMART Signal Technologies, Inc., a Minnesota-based private company that could commercially benefit from the results of this research. These relationships have been reviewed and managed by the University of Minnesota in accordance with its Conflict of Interests policies.

Table of Contents

EXECUTIVE SUMMARY 1
CHAPTER 1 1
INTRODUCTION 1
1.1 Background and Relevant Work 1
1.2 Research Objectives 3
1.3 Organization of This Report 3
CHAPTER 2 4
FRAMEWORK OF FINE-TUNING SIGNAL PARAMETERS AND ALGORITHMS TO DIAGNOSE OPERATIONAL PROBLEMS 4
2.1 Introduction 4
2.2 Data Collection Unit 5
2.3 Diagnosis Framework and Methodology 7
2.3.1 Offset Diagnosis Module 8
2.3.2 Green Split Diagnosis 9
2.3.3 Cycle Length Diagnosis 10
2.4 Field Case 11
2.5 Conclusions 15
CHAPTER 3 17
OFFSET EVALUATION AND FINE-TUNING 17
3.1 Background about Time Space Diagram 17
3.2 Constructing Link TS-Diagram 18
3.3 Validation of TS-Diagram 23
3.3.1 Case 1: TH 55 23
3.3.2 Case 2: TH 13 25
3.4 Fine-Tuning Using TS-Diagram with Offset and Lead-Lag Sequence 26
3.5 Conclusions 31
CHAPTER 4 GREEN SPLITS EVALUATION AND FINE-TUNING 32
4.1 Measure of Effectiveness for Green Splits 32
4.1.1 V/C Ratio 32
4.1.2 Queue Service Time (QST) 33

4.1.3 Utilized Green Time and Slack Green 34
4.2 Green splits rebalancing based on UGT 35
4.3 Split Fine-tuning Example 36
4.4 Conclusions 38
CHAPTER 5 39
OPTIMIZING AND FINE-TUNING TIME OF DAY TRANSITIONS 39
5.1 Introduction 39
5.2 Methodology 40
5.2.1 Delay at Non-coordinated Phases 41
5.2.2 Delay at Coordinated Phases 41
5.2.3 Estimating Duration Length for Actuated Signals 42
5.3 Case Study 44
5.3.1 Estimating green time 45
5.3.2 Fine-tuning TOD based on delay 47
5.4 Conclusions 50
CHAPTER 6 51
CONCLUDING REMARKS AND FUTURE RESEARCHES 51
6.1 Concluding Remarks 51
6.2 Limitations and Future Research 52
REFERENCES 53

List of Tables

Table 2.1 Comparison of Observation and Optimization Results 12
Table 2.2 Average GUR for Intersection 0403 and intersection 0404 14
Table 3.1 Before-After comparison of delay from SMART-Signal System 31
Table 5.1. Performance comparison between original and modified schedules 50

List of Figures

Figure 2.1 Architecture and snapshots of DCUs 6
Figure 2.2 Illustration of field installation of Type 2 DCU and data sample 7
Figure 2.3 Implementation procedures for traffic signal parameter diagnosis 8
Figure 2.4 PCD of three instrumented sites 13
Figure 2.5 Layout and ring diagrams for instrumented intersections 14
Figure 2.6 Optimized intersection cycle length 15
Figure 2.7 Estimated optimal bandwidth efficiency with varied cycle length 15
Figure 3.1 Example of TS-Diagram 17
Figure 3.2 Screenshot of Synchro TS-Diagram 18
Figure 3.3 Illustration of queuing at intersection with QOD 21
Figure 3.4 Example of CFP 22
Figure 3.5 Illustration of car following and dummy vehicle. 23
Figure 3.6 Layout and TS-Diagram for TH 55 24
Figure 3.7 Estimated CFPs VS Observed CFPs for EB (Up) and WB (Down) traffic 25
Figure 3.8 TS-Diagrams for selected intersections on TH 13 26
Figure 3.9 Offset reference point and combinations of lead lag sequence 27
Figure 3.10 TS-Diagrams for selected intersections on TH 13 with average (left) and relatively congested conditions (right) 28
Figure 3.11 Before-After comparisons of TS-Diagrams with relatively congested condition 30
Figure 3.12 Before-After comparison of maximum queue length from SMART-Signal System 31
Figure 4.1 Example of traffic events from long detector at stop bar 33
Figure 4.2 Illustration of QST 34
Figure 4.3 Example of QST and UGT calculation 35
Figure 4.4 Intersection layout and ring-and-barrier diagram of the signal timing 36
Figure 4.5 Green Time VS Utilized Green Time 37
Figure 4.6 Ring-and-barrier diagrams with UGTs 38
Figure 5.1 Illustration of delay calculation at coordinated phases 42
Figure 5.2 Green duration depending on cycle volume without pedestrian calls (left) and with pedestrian calls (right) 43
Figure 5.3 Cycle green duration depending on cycle volume (A) and average green duration depending on average volume (B) 44
Figure 5.4 Layout of interested segment from Google Map (Left) and layout of simulated road network in VISSUM (Right) 45

Figure 5.5 Intersection layout and Ring-and-Barrier Diagram at Int. TH13 & Portland Ave. 46
Figure 5.6 Estimated green time VS observed green time depending on 15 minutes volume (A) phase 1, (B) phase 4, (C) phase 5 and (D) phase 8. 47
Figure 5.7 Estimated green time VS observed green time for coordinated phases 47
Figure 5.8 Main-street volume over time of day 48
Figure 5.9 Total delays over TOD for the two timing plans..... 49
Figure 5.10 Delay at the main street for the two timing plans..... 49

EXECUTIVE SUMMARY

Maintaining an efficient traffic signal operation is a challenging task for many traffic management agencies. Due to intensive labor costs required in the signal retiming process, most of the traffic signals in the US are retimed once every 2-5 years. However, it has been shown in the past that traffic delay increases 3-5% per year simply because the timing plans are not kept up to date. For many resource-constrained agencies, it would be desirable to reduce signal re-timing costs by automating all or a portion of the manual process. The research takes one step toward this direction.

In this research, we develop a performance visualization and fine-tuning tool for arterial traffic signal systems, aimed at reducing the labor cost for signal retiming and to help identify adjustment opportunities. Using high-resolution event-based traffic data collected by the SMART-Signal System, a set of theoretically sound, while easy-to-use algorithms are proposed to refine traffic signal systems for coordinated arterials.

In detail, a framework to diagnose operational problems regarding cycle lengths, green splits and offsets is first developed. Then algorithms for offsets and green splits fine-tuning are proposed. To fine-tune signal offsets, a practical procedure to construct the time space diagram (TS-Diagram) to visualize the progression quality on arterials is proposed and validated using the field data. A field experiment is carried out to illustrate how decisions regarding changes can be made by intuitively evaluating the TS-Diagram. For green splits, an adjusted measure of effectiveness (MOE), the utilized green time (UGT), is proposed for performance evaluation. The information is further tabulated in a ring-and-barrier diagram to facilitate evaluation. Moreover, a practical procedure for time of day (TOD) transitions is proposed to generate optimal timing plan schedules. The procedure is validated by simulation experiment.

The proposed algorithms are intended to partly automate the signal retiming process, thus help agencies to reduce labor costs during the retiming process. The algorithms also would be suitable to help engineers refine the traffic signal systems periodically and hence maintain efficient signal operations in a timely manner.

CHAPTER 1
INTRODUCTION

It is commonly understood that traffic delay increases 3-5% per year simply due to the fact that the timing plans are not kept up to date. The signal retiming, however, is only conducted once every 3 to 5 years because it involves largely manual processes. For many resource-limited agencies, it would be desirable to reduce the labor-intensive signal re-timing process by using algorithms for automated or semi-automated updating of the signal parameter settings. Previous attempts have largely failed due to the unavailability of the field performance data, and the need for calibrating parameters of embedded traffic models. However, over the past decade or so, there have been significant advances in data collection and performance measurement technology (for example, the SMART-SIGNAL system developed at the University of Minnesota), such that a fresh look at automated timing plan generation is warranted.

The goal of this research is to develop methods to reduce labor costs associated with signal retiming process by using detector and signal data, and thus to automate, at least partly, the generation of coordinated timing plan on signalized arterials. This project aims to extend SMART-SIGNAL's capability for automatic diagnosis of operational problems and fine-tuning signal control parameters. Based upon large volume of traffic signal performance data collected by the SMART-SIGNAL system, we propose systematic diagnosis and optimization tools for signal parameter optimization and fine-tuning. These data-driven algorithms and tools are aiming at extending the life of an existing signal timing plan by fine-tuning the parameters and reduce the frequency and expense of manual work for signal retiming.

1.1 Background and Relevant Work

In the literature, traffic signal retiming plans typically require labor/cost-intensive field data collections (volume, queue, delay, etc.). Gordon (2010) surveyed agencies' practices regarding traffic signal retiming and summarized that traffic movement data used in existing signal retiming processes are usually collected manually. Because data collection is a labor/cost-intensive process, traffic signal retiming is usually performed in a 3 to 5-year time interval. Koonce et al. (2008) suggested a shorter time interval for signal retiming if there are significant changes in traffic volumes or roadway conditions. However, as indicated by Gordon & Braud (2009), it is more appropriate to review the intersection performance in a higher frequency, especially for performance-oriented operation. Limited by the level of resources, existing signal retiming processes are not suitable for high frequency adjustment. With limited resources, some researchers (e.g., Henry, 2005) provided compromised procedures to accomplish retiming at a lower cost but with degradation in performance. Smaglik et al. (2007) proposed to use a controller to collect data for signal retiming; however, algorithms that can use the data to optimize the signal parameters are not provided. An automated signal retiming process is highly desired to identify operational problems and suggest solutions simultaneously.

It is not surprising that very few studies can be found in the literature focusing on automatic generation or fine-tuning of signal control parameters. It is partly due to the complexity of the problem and partly due to the lack of advanced techniques to collect large-scale and high-resolution traffic signal data. Therefore, most of previous studies on updating

signal parameters were developed with specific objectives. For example, Khosla & Williams (2006) investigated how the adjustment of green time impacts the saturation flow change; Denney et al. (2009) tested the relationship between the length of green and headway as well as the relationship between cycle length and throughput; Yin et al. (2007a) studied how to fine-tune offsets in semi-actuated coordinated systems to improve the signal control system performance; Wood et al. (1994) provides a simple decision tree based approach to diagnose offset problems under congestion. Since these studies were problem-specific, they did not provide a general methodology that can detect operational problems of traffic signal and provide potential solutions.

Most existing studies on automated signal updating have been focused for developing adaptive traffic signal control using real-time traffic data, and very few of studies have examined the use of archived traffic signal data to fine-tune signal parameters (Yin et al. 2007b). Smith et al. (2002) developed a clustering algorithm to determine appropriate Time of Day (TOD) intervals using archived 15-minute volume data for traffic signal operations. Yin et al. (2007a) presented the concept and implementation of an offline offset refiner using archived signal status data. Later, Yin (2008) established robust signal timing settings based upon archived traffic conditions at signalized intersection. However, in these studies, either volume data or signal status data was used, but not both. Therefore, these approaches do not capture the inherent dependency between traffic flow and traffic control.

On the other hand, the University of Minnesota has developed and implemented the SMART-SIGNAL: Systematic Monitoring of Arterial Road Traffic Signals, which is an arterial data collection and performance measurement system. In the SMART-SIGNAL system, a complete history of traffic signal control, including all signal events such as vehicle actuations on detectors and signal phase changes, is archived and stored. Using the high resolution event-based data, SMART-SIGNAL can provide a set of performance measures, through monitoring the maximum queue length, intersection delay, and level of service at the single intersection level and reporting travel time, speed, and average number of stops at the arterial level. The event-based signal data are being collected in a 24/7 mode and then immediately archived in the SMART-SIGNAL system, thus yielding a tremendous amount of field data available for diagnosis of problems and refining signal plans parameters. The SMART-SIGNAL system has been installed at 11 intersections along France Avenue in Hennepin County, Minnesota in February 2007, and at six intersections along Trunk Highway 55 of Mn/DOT in February 2008. The updated SMART-SIGNAL system with redesigned hardware and software for the TS-2 controller cabinet has also been implemented and tested at 13 intersections on Trunk Highway 13 since December 2011.

The data collection and performance measurement effort with the SMART-SIGNAL system serves as a solid foundation for this proposed work. Using the large volume of data archived by SMART-SIGNAL system, in this work, we further develop the SMART-SIGNAL system and propose a set of data-driven algorithms and tools to investigate the archived data and identify potential operational problems, and thus fine-tune and optimize signal control parameters correspondingly.

1.2 Research Objectives

This work has a high priority to maximize the investment in traffic signal systems, particularly with declining funding to add roadway capacity. Since outdated signal plans will increase travel delays, fuel consumption, vehicle emissions, and accident rates, a frequent adjustment of signal timing plans is desired. A system for monitoring signal timing performance and identifying improvement opportunities is ideal to reduce the cost for signal retiming, and thus improving the system performance of signalized arterials.

In addition, this work will serve as a natural extension of the existing developments of the SMART-Signal system. It may also bring innovative changes to the state-of-the-practice because of the anticipated significant reductions in the frequency and effort needed for manual signal re-timing. Based on continuous data collection and processing, the proposed algorithms can easily help engineers refine the signal system periodically without much labor costs, and hence significantly reduce the expense of traffic signal operations.

There are four main tasks for this project. The first task of this project focuses on developing a framework for systematic parameters optimization regarding offsets, green splits and cycle length. In the second and third tasks, we will get into more details regarding offsets and green splits fine-tuning. The last task focuses on optimizing signal plan schedules for time of day (TOD) traffic signal operations.

1.3 Organization of This Report

The rest of the report is organized as following. First, in Chapter 2, we will briefly discuss the data collection and then introduce a framework of simple fine-tuning algorithms for cycle length, offset, and splits. Then, in chapter 3, we will discuss in details about offset fine-tuning procedure with focus on generating and evaluating time space diagram using detector and signal data. In chapter 4, the procedure to fine-tune green splits will be discussed in details. Chapter 5 introduces a data-driven algorithm to fine-tune the TOD transition points among different time plans for coordinated arterials. Finally, concluding remarks and future researches are documented in Chapter 6.

CHAPTER 2
FRAMEWORK OF FINE-TUNING SIGNAL PARAMETERS AND ALGORITHMS TO DIAGNOSE OPERATIONAL PROBLEMS

In this chapter, we will briefly describe the data collection unit, which is implemented in the SMART-Signal system, and then introduce the framework for optimizing and fine-tuning offsets, splits and cycle lengths (Zheng et al., 2013).

2.1 Introduction

Efficient traffic signal operation is vital for smoothing traffic flows in signalized network and greatly beneficial for road users. Conventionally, traffic signal settings are determined based on manually collected field data (Day et al., 2009). Due to the intensive labor required, although signal retiming has a very high benefit/cost ratio (Koonce et al., 2008), most of the traffic signals in the US are retimed once every 3-5 years, or even longer (Gordon, 2010). Although detectors are widely implemented for signalized arterials, the majority of agencies operating traffic signal system do not archive and analyze traffic performance data frequently (Balke & Herrick, 2004; Balke et al., 2005; Liu & Ma, 2009;). Such practice may miss the opportunities for operational improvements and result in unnecessary delays.

One of the major obstacles to improve the practice is the lack of data collection capability and a convenient performance monitoring tool for traffic signal systems. Although real-time performance measures for freeway travel speeds and travel time are commonly available nowadays, they are still relatively new for signalized arterials (Day et al., 2010a). Recently, increasing research interests were found in performance measure for traffic signal systems using high-resolution event-based data, and encouraging results were achieved. The "event" here refers to vehicle-detector actuation and de-actuation and traffic signal phase changes, all measured in high resolution time intervals. Appeal of such event-based data over aggregated data includes: (a) performance measures based on larger time intervals (per phase, cycle, hour, and day, etc) can be easily calculated and (b) event-based data on individual vehicle level helps to make more accurate and detailed traffic state evaluation, particularly during congested traffic condition.

To the best of our knowledge, researchers from the Texas Transportation Institute (TTI) made the first attempt to retrieve traffic event data from existing traffic detection systems. Their prototype system, the Traffic Signal Performance Measurement System (TSPMS) can automatically collect traffic event data and generate performance measures for individual intersections (Balke et al., 2005; Sunkari et al., 2011). Using event-based data, Smaglik et al. proposed methodologies for calculating vehicle-actuated controller performance measures (Smaglik et al., 2007). It has also been demonstrated that Webster's work (Webster, 1958) can be applied easily with the same type of data to identify opportunities to shorten the cycle lengths and correct phase failures (Day et al., 2010a). In a recent work by Day et al. (2010b), the Purdue Coordination Diagram (PCD) is developed to visualize event-based data, and it has been shown as a convenient tool to help adjusting offsets. Based on the same type of high-resolution data, the University of Minnesota researchers developed the Systematic Monitoring of Arterial Road Traffic and Signals (SMART-SIGNAL) System that can accurately estimate arterial travel time and intersection queue length in real time (Liu & Ma, 2009; Liu et al., 2009; Gordon 2010;). Research by Wu et al. (2010) demonstrated that by using high resolution event-based data, oversaturation at signalized intersections could be identified.

Utilizing the event-based traffic data, in this chapter, we propose a performance diagnosis tool for arterial traffic signals. The tool consists of a data collection system deployed within the signal cabinets and a data analysis package in a remote center. Given that most of the current traffic signal cabinets are not capable of collecting event-based traffic data, an event-based data collection unit (DCU) is developed to overcome this issue. An easy-to-implement framework for evaluation of offset, green split and cycle length is then developed based on proper measure of effectiveness (MOE) with corresponding optimization strategies. It is our hope that the proposed data-driven performance diagnosis tool will improve the state-of-the-practice on traffic signal operations by automatically identifying necessary changes to traffic signal timing parameters.

2.2 Data Collection Unit

Although detectors are commonly available in many signalized intersections, further modifications are required for existing traffic signal system to retrieve event-based data, as standard traffic signal controllers normally aggregate data in 5-60 minutes bins. To address the issue of the non-standardized interface of controller MOE output, Bullock & Catarella (1998) developed the controller interface device (CID) that can interface the signal controller with a personal computer recording signal events and detector events in real time. TTI's TSPMS extended CID with a data acquisition card to obtain event-based data from NEMA (National Electrical Manufacturers Association) TS1 cabinets. The data is further processed by an industrial computer within the cabinet. For NEMA TS2 cabinets, an enhanced bus interface unit (BIU) is used to interface with the Synchronous Data Link Control (SDLC) bus of the controller, and the industrial computer is replaced by a rugged laptop for easier user interaction (Balke et al., 2005; Sunkari et al., 2011). The National Institute for Advanced Transportation Technology (NIATT) of the University of Idaho developed a data logging device (DLD) for recording high resolution traffic event data, adopting similar architecture of data collection system as in the TSPMS for TS1 cabinets (Ahmed & Brain, 2008). Although SDLC bus based interface is recognized, the connection of DLD for TS2 cabinet is still based on harness cable connection matrix on the back panel within the signal cabinet.

As mentioned by Smaglik et al. (2007), Econolite ASC/3 Controller features a data logger capability that can retrieve event-based data. Events are recorded with 0.1 sec time-stamp, and stored as binary-formatted files. The raw data can be stored within the controller, and uploaded via FTP. However, vender based data collection solution, such as Econolite ASC/3 Data Logger, is still far from standardization and is not convenient for agencies with controllers from various venders. Although efforts can be seen recently from the vender side to enhance event-based data collection capability within the controller, we expect that the progress for a vendor-dependent solution will be gradual and time consuming.

The Data Collection Unit (DCU) we developed for the SMART-Signal system is a low cost add-on module to enhance traffic cabinets with event-based data collection capabilities. There are two types of DCUs: Type 1 DCU with pin-to-pin interface and Type 2 DCU with SDLC interface, to interface with TS1 and TS2 cabinets, respectively. The DCU can automatically archive event-based traffic data on a local storage media card and send the data to a remote center using Ethernet based communications. Based on the embedded system technology, the DCU is compact and reliable to be equipped in traffic signal cabinets. The general architecture and snapshots of two types of DCUs are shown in **Figure 2.1**. More details related to DCU

design can be found in a recent research report funded by Minnesota Department of Transportation (Liu et al., 2013).

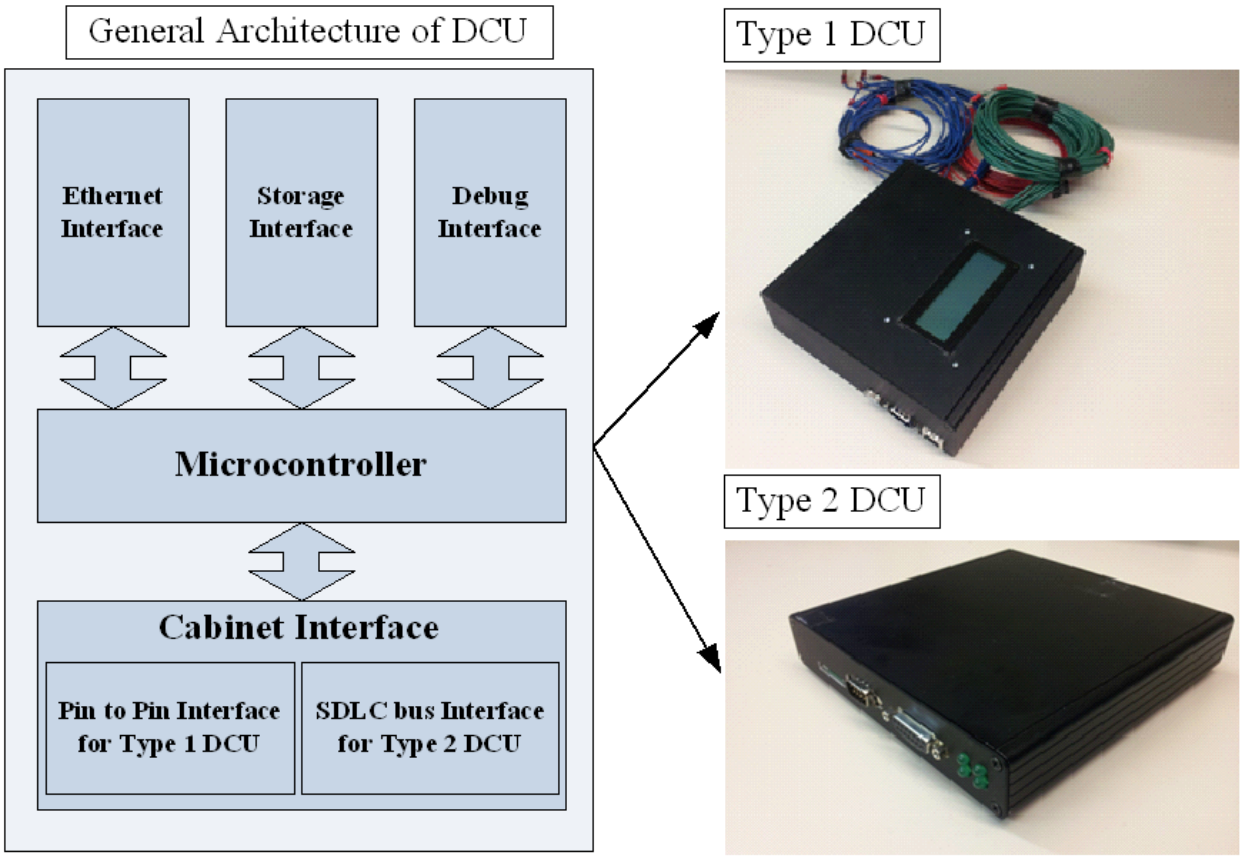

Figure 2.1 Architecture and snapshots of DCUs

The sample of data collected by DCUs is illustrated in **Figure 2.2**, along with a Type 2 DCU installed at intersection of Nicollet Avenue & TH13 in Burnsville, Minnesota. Detector events are recorded with detector actuation time, event duration length and detector ID. Traffic signal events are recorded with signal phase start time, duration length, signal status and phase ID. The timing in Type 1 DCU is synchronized with the central server. Since Type 2 DCU interface with controller by SDLC bus directly, it synchronized with controller from the controller broadcasting time (NEMA, 2003).

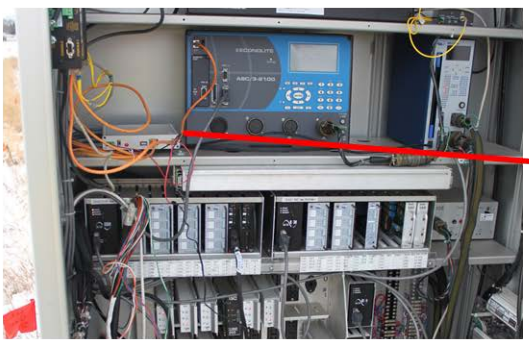

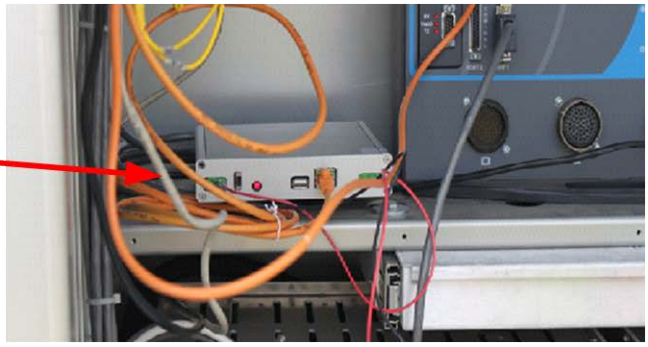

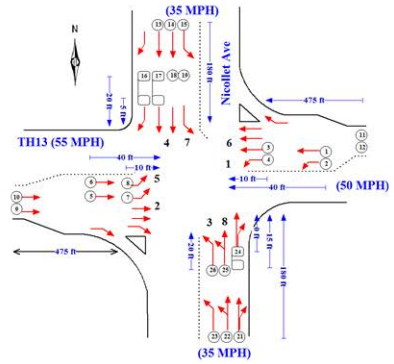

Detector occupation event

Start Time of Detector "ON"	Detector ID	Occupied Duration(Sec)
05:00:16.400	13	0.321
05:00:21.157	10	0.403
05:00:20.989	16	1.369
05:00:22.580	9	0.403

Signal Event

Start Time	Signal Status	Phase	Duration(Sec)
05:00:16.800	G	3	9.800
05:00:26.600	Y	3	4.000
05:00:33.100	G	4	10.300
05:00:43.400	Y	4	4.000

Figure 2.2 Illustration of field installation of Type 2 DCU and data sample

2.3 Diagnosis Framework and Methodology

While performance measures based on various intervals can be calculated with event-based data, cycle-by-cycle and phase-by-phase performance measures are selected for analysis due to their intrinsic meaning for traffic signal systems (Day et al., 2010a). Three modules are included for evaluation: the offset, green split and cycle length diagnosis modules. Since cycle length is commonly shared by multiple intersections within a signal timing zone, changes of cycle length will lead to necessary adjustments of associated green splits and offsets. Similarly, adjustments of green splits of coordinated phases will require additional offset adjustments at adjacent intersections. On the other hand, changes of offsets normally do not require subsequent changes of green splits and cycle length. Because of this causal relationship, the diagnosis procedure is proposed to be hierarchical, as indicated in **Figure 2.3**. To start, the user can select one of the parameters for evaluation. Then, the tool will evaluate selected parameters in the order indicated in **Figure 2.3**. For example, if a user selects cycle length to start with, subsequent diagnosis and fine tuning of green splits and offsets will need to be done. The implementation of diagnosis also needs to be done iteratively with implementing parameter changes until no further fine-tuning is needed.

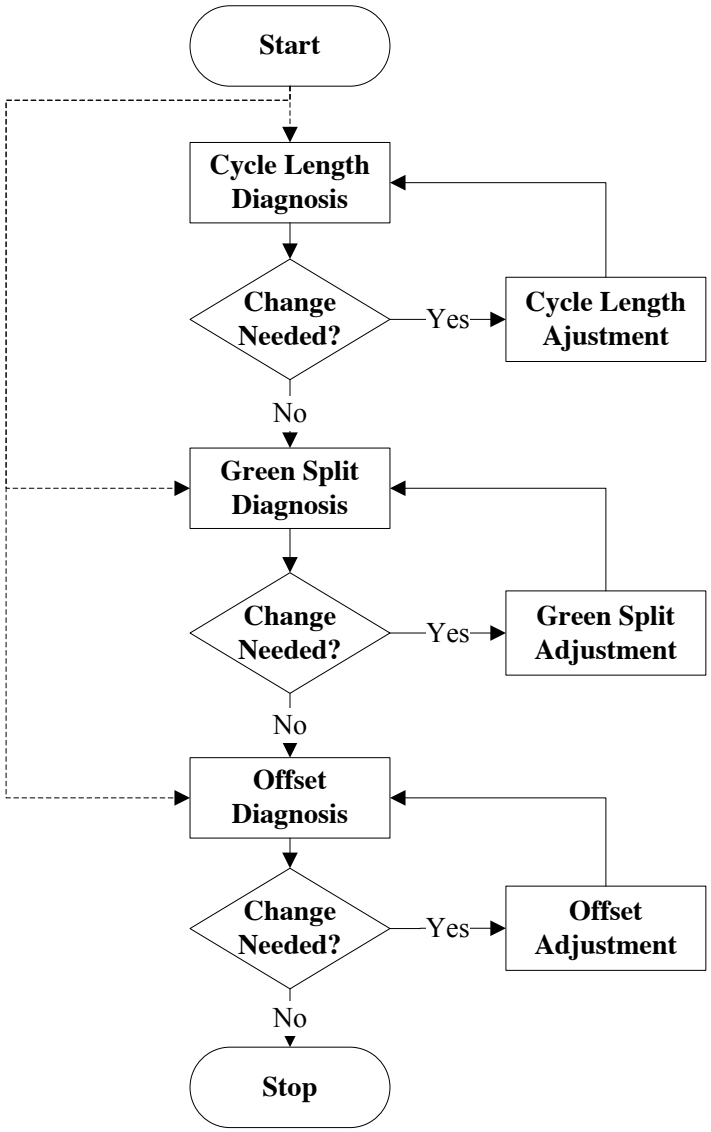

Figure 2.3 Implementation procedures for traffic signal parameter diagnosis

2.3.1 Offset Diagnosis Module

Classical measures of effectiveness (MOE) for signal coordination include travel time, vehicle stops, arrival type, arrivals on green (AOG), percent arrivals on green (POG), and bandwidth (Day et al., 2009; Balke & Herrick, 2004; Smaglik et al., 2007; TRB, 2000). Although arterial travel time and vehicle stops are intuitive to drivers, AOG, POG and bandwidth are more useful from traffic operation perspective. Using data from setback detectors, AOG can be obtained directly. Based on AOG, the POG can be further calculated by:

$$POG = \frac{AOG}{Arrivals\ over\ Cycle} \tag{2.1}$$

Another widely used MOE for offset optimization is the bandwidth, defined as "maximal green time for a designated movement to pass through a corridor" (Koonce et al., 2008). It can be further characterized as link bandwidth for two consecutive intersections and arterial bandwidth for the entire corridor.

Optimal offset for a specific MOE can be easily found for one-direction coordination. For two-direction coordinated arterials, the trade-off in opposite directions makes it difficult to find an optimum. Considering arterial bandwidth, well-established offset optimization models include the famous MAXBAND and its derivatives (Morgan & Little, 1964; Little et al., 1981; Gartner et al., 1990). One of the disadvantages of MAXBAND is that the methodology does not utilize the vehicle arrival data effectively. Recent studies by Day et al. (2010b), and Day & Bullock (2011) extended the classical combination method (CM) (Gartner & Little, 1975) with vehicle arrivals from setback detectors and illustrated the Link Pivot Combination Method (LPCM) for offset optimization. Different from MAXBAND with the objective to maximize bandwidth through arterials, CM assumes that changes of signal offset only make an impact to its nearest downstream intersections. Such simplification helps to change optimization for a corridor into sequential optimizations based on links, and makes it convenient to incorporate vehicle arrival information. In fact, CM for a signalized corridor can be stated by a simple rule: considering two phases that share a same link, if vehicles for a signal phase arrive relatively early than green start while vehicles for another phase arrives relatively late than green start, then an improvement can be made to accommodate both by offset shifting. For the details of the methodology, the readers can refer to (Day & Bullock, 2011). This rule is used in the offset diagnosis module, with the criteria:

A change of offset is needed if: the difference between the AOG optimized by CM and observed AOG exceeds an acceptable range.

2.3.2 Green Split Diagnosis

For green split, one of the most widely used MOE is the volume to capacity ratio (v/c ratio) that indicates saturation level of a specific signal phase (Day et al., 2010a; TRB 2000). It can be calculated by:

$$X_i = \frac{V_i}{s_i x_i} \tag{2.2}$$

Where:

$X_i :=$ v/c ratio of phase i,

$V_i :=$ Flow rate of phase i,

$s_i :=$ Saturation flow rate of phase i,

$x_i = \frac{g_i}{C} :=$ Green split of phase i,

$g_i :=$ Effective green time of phase i, and

$C :=$ Cycle length.

When applying Equation (2.2), vehicle counting accuracy using loop detectors needs to be taken into consideration. The accuracy for vehicle-counting reduces with stop bar detectors that are mostly used for detection of vehicle presence. For presence detectors, the miscounting may become significant due to relatively short spacing between consecutive vehicles. It becomes even worse when long or sequential detectors are implemented (Lawrence et al., 2006). Recent research has shown that the Green Occupancy Ratio (GOR), sum of detector occupation time during green over green duration time, can be used as a reasonable alternative for v/c ratio after calibration (Smaglik et al., 2011). The GOR can be calculated by:

$$GOR_i = \frac{O_g}{g_i} \quad (2.3)$$

Where:

O_g = Total duration time that detector is occupied during a green interval.

Thus, for intersections with both setback detectors and stop bar detectors, we propose the adjusted performance measure for green split diagnosis accounting for such miss-counting phenomena, the Green Utilization Ratio (GUR) U_{i} as:

$$U_i = Max(X_i, GOR_i) \quad (2.4)$$

The rule of thumb for determining green splits is to assign them proportional to demands (Webster, 1958). Unbalanced GURs indicate improvement opportunities especially when some phases are oversaturated. Therefore, the criteria of green split diagnosis based on GUR, is proposed as:

A change of green splits is needed if: GURs are not balanced, with oversaturated phases indicated by high GURs.

2.3.3 Cycle Length Diagnosis

Cycle length is probably the most important parameter for traffic signal system (Gartner & Little, 1975). Longer cycle lengths usually increase intersection capacity. On the other hand, shorter cycle lengths reduce delays for unsaturated phases. Shorter cycle lengths that do not exceed 100-120 seconds are typically preferred since marginal capacity gain from increasing cycle length is rather modest (Koonce et al., 2008; TRB, 2000). Conventionally, the maximum and minimum cycle lengths of each intersection using Webster's formula (Webster, 1958) are selected as the common cycle lengths for coordinated arterials. This is mostly from capacity management consideration. For fine-tuning of an implemented cycle length, the impacts on progression increase the concerns for changes. Thus, the proposed cycle length diagnosis procedure includes two parts of evaluations: intersection capacity evaluation based on Webster's formula and coordination evaluation based on bandwidth. As mentioned before, the change of cycle length will result in needs for subsequent adjustments of green splits and offsets. If diagnosis and fine-tuning of green splits and offsets are not performed subsequently, the cycle length change should not be implemented.

Intersection Capacity Evaluation

For an evaluation of individual intersection capacity, the Degree of Saturation X_c based on GUR is selected as an indication of overall saturation. The formula for X_c (Day et al., 2010a) is given by:

$$X_c = \sum_i (Ux)_{ci} \left(\frac{C}{C-L}\right) \quad (2.5)$$

Where:

L: = Lost time, and

$\sum_i (\cdot)_{ci}$ = Summation over critical phases.

In the formula, the critical phases are phases that serve critical movement (Koonce et al., 2008; Day et al., 2010a; TRB, 2000). For a typical eight phase dual ring signal diagram, the following calculation can be used:

$$\sum_i (Ux)_{ci} = \max[(Ux)_{12}, (Ux)_{56}] + \max[(Ux)_{34}, (Ux)_{78}] \quad (2.6)$$

Where: $(Ux)_{ij} = U_i x_i + U_j x_j$.

Based on X_c, the optimal cycle length by Webster's model, C_o, is calculated as:

$$C_o = \frac{1.5L+5}{1-X_C} \quad (2.7)$$

Coordination Evaluation

With cycle length changes, the simplified treatment for changes of arrivals based on CM is not appropriate. Although modified treatment of arrivals can be applied, it does not necessarily benefit the analysis considering the subsequent adjustments of green splits and offsets. As an alternative, we only focus on utilizing signal information, and use bandwidth efficiency (Koonce et al., 2008) as MOE for coordination evaluation regarding cycle length change. The formula for bandwidth efficiency is:

$$E = \frac{(B+\bar{B})}{2C} = \frac{1}{2}(b + \bar{b}) \quad (2.8)$$

Where:

$E :=$ bandwidth efficiency,

$B, \bar{B} :=$ the bandwidths in forward and reverse directions, and

$b, \bar{b} :=$ normalized bandwidths, which is bandwidths divided by cycle length, in forward and reverse directions.

Based on bandwidth efficiency, MAXBAND can be used to optimize offset with different cycle lengths and evaluate the best possible coordination parameters. The criteria for cycle length diagnosis is proposed as:

A change of cycle length is needed if: Webster's model yields a significantly different cycle length, while the change of bandwidth efficiency with the new cycle length is acceptable.

2.4 Field Case

With support from MnDOT, thirteen sets of Type 2 DCUs were implemented in intersections on TH13. For illustrative purposes, only part of network with nontrivial diagnosis results is highlighted here.

Offset Diagnosis

Three of the instrumented intersections (**Figure 2.4**), labeled with 0407 - 0409, were selected with data collected during 10:00 AM-06:00 PM on Saturday April 14th, 2012 to evaluate offsets of a weekend signal timing plan. Phases 2 and 6 are coordinated phases. Since phase 6 at intersection 0407 and phase 2 at intersection 0408 share a link, arrivals of these two phases need to be considered jointly. The same rule applies for phase 6 at intersection 0408 and phase 2 at intersection 0409. The optimization results based on CM are listed in **Table 2.1**. Even though relatively high POGs (>70%) are observed, optimization based on CM still shed light on

improvement opportunities. The main improvement is at intersection 0408 phase 2 with largest increase of AOG, however, with reduction at intersection 0407 phase 6.

Table 2.1 Comparison of Observation and Optimization Results

		0407 Phase6	0408 Phase2	0408 Phase6	0409 Phase2
POG	Observed	77.86%	73.86%	82.89%	74.34%
	Optimized	73.94%	80.90%	86.96%	77.15%
	Absolute Change	-3.922%	7.03%	4.08%	2.80%
AOG (Vehicle/Lane)	Observed	3891	4845	4038	4458
	Optimized	3695	5307	4237	4626
	Absolute Change	-196	462	199	168

In **Figure 2.4**, qualitative investigation using PCD (Day et al., 2010) reveals some further details of potential improvements. In each of the six sub-figures in **Figure 2.4**, the horizontal axis shows time of day, and vertical axis shows time within a cycle. The green, yellow and red lines represent start times of green, yellow and red signal respectively. Each dot indicates a vehicle arrival, and major arrivals are circled by ellipses with red dash. Four red arrows indicate estimated arrivals change directions with optimal offset adjustments. As shown in the figure, major arrivals of phase 2 at intersection 0409 arrived late regarding the green start, while at intersection 0408 phase 6, the secondary platoon arrived early regarding green start. This can be improved with offset adjustment. Similar opportunity exists for improvement at intersection 0408 phase 2 and 0407 phase 6 as well.

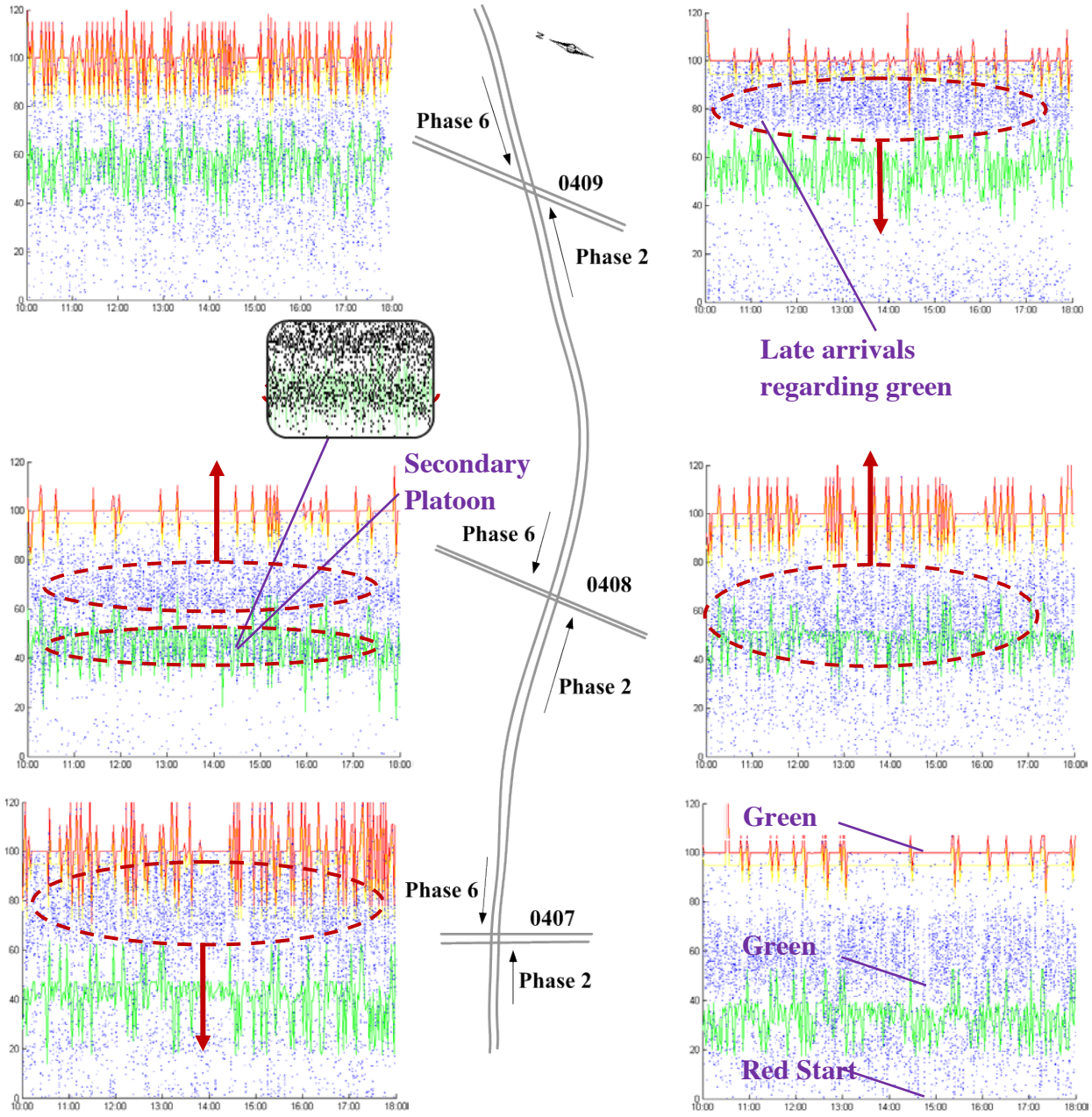

Figure 2.4 PCD of three instrumented sites

Green Split and Cycle Length Diagnosis

Figure 2.5 shows another two instrumented intersections on TH 13, indexed 0403, 0404, with corresponding signal timing ring diagrams for weekday morning peak hours. The diagnosis results here are based on data collected on Monday, April 9th 2012 from 6:30-8:30 AM.

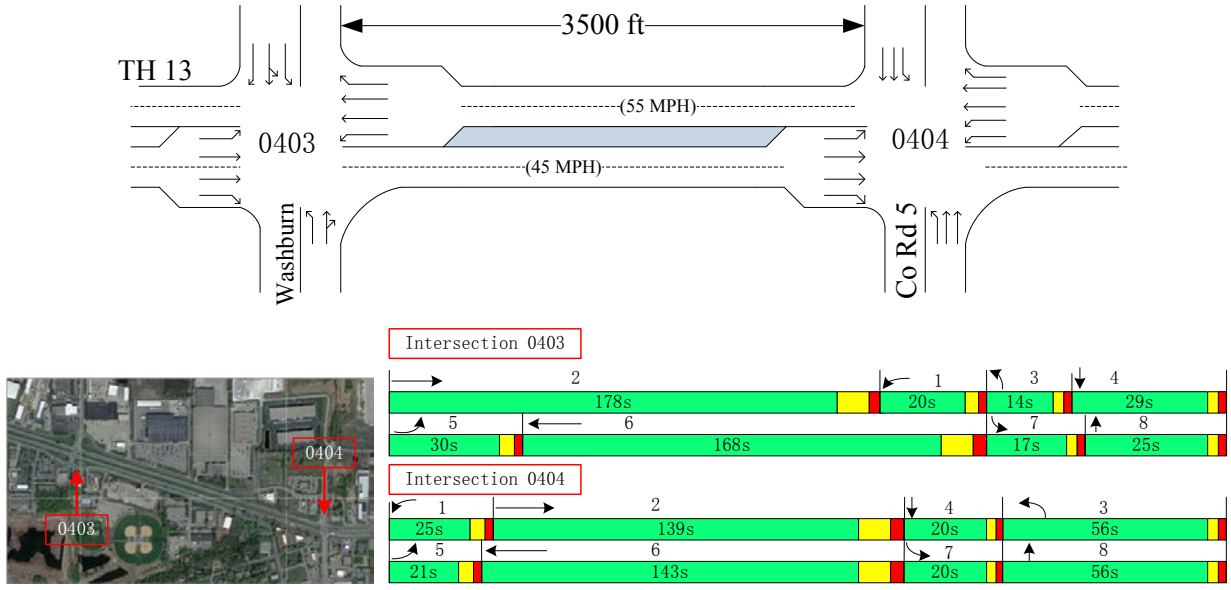

Figure 2.5 Layout and ring diagrams for instrumented intersections

Green Split Diagnosis

Table 2.2 shows the average GURs for both intersections, with critical phases indicated in red. In general, intersection 0404 is more saturated than intersection 0403. In intersection 0403, relatively low GURs of phase 7 and 8 are observed with high GURs of phase 1 and 2, indicating chances for the rebalancing of green splits. A similar situation occurs in intersection 0404, with highest GUR of 81% of phase 1, while phase 8 has only utilized 18% percent of green time assigned. Opportunity and necessity for green split changes of both intersections are therefore justified.

Table 2.2 Average GUR for Intersection 0403 and intersection 0404

(Red color indicated it is a critical phase)

Phase	1	2	3	4	5	6	7	8
0403	70%	55%	54%	30%	56%	46%	38%	57%
0404	81%	74%	17%	31%	52%	60%	51%	18%

Cycle length diagnosis

Intersection Capacity Evaluation **Figure 2.6** plots optimal cycle lengths over an evaluation period using Webster's formula. The optimal cycle lengths are around 50-120 seconds, much shorter than the operating value of 240 seconds. The need for cycle length changes is indicated.

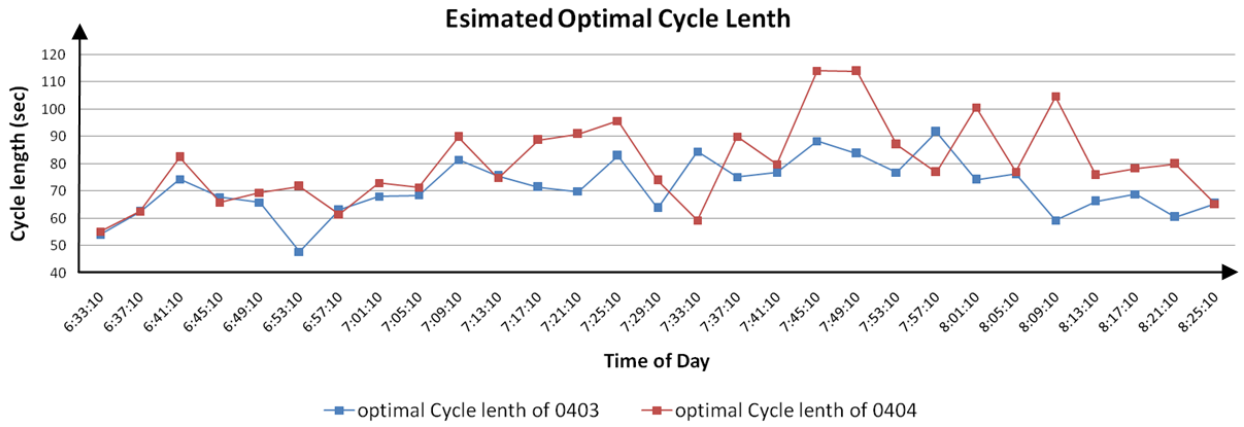

Figure 2.6 Optimized intersection cycle length

Coordination Evaluation In the next step, the impact on coordination with cycle length changes was evaluated using MAXBAND. The average values of the observed green splits were used to calculate maximal bandwidth efficiency with cycle lengths ranging from 60 to 240 seconds. As shown in **Figure 2.7**, with a shorter cycle length around 70-130 seconds, bandwidth efficiency can be improved from the one achieved by the current cycle length of 240 seconds.

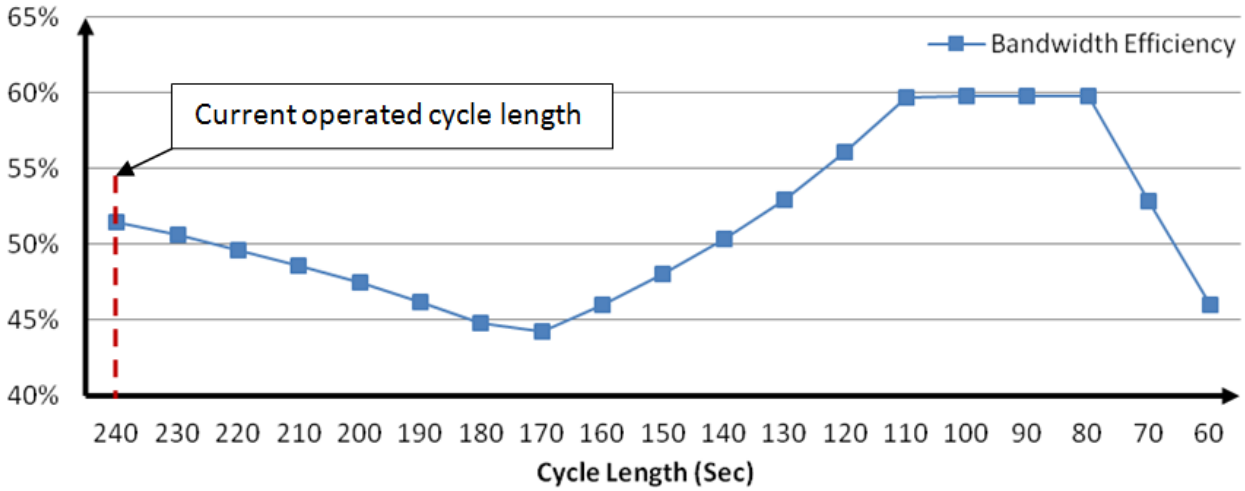

Figure 2.7 Estimated optimal bandwidth efficiency with varied cycle length

Therefore, it would be reasonable to conclude that a shorter cycle length around 100-120 seconds can help to reduce delays on non-coordinated approaches with only minor impact on coordination for selected intersections. The need for change of cycle length at selected intersections is justified.

2.5 Conclusions

Although detectors for signalized arterials are available in general, the lack of data collection and analysis could result in inefficient operation of traffic signal system and unnecessary delays. The tool presented in this chapter is intended to make up for such inefficiency. A flexible and low cost add-on module, the DCU, is developed to enhance current traffic signal cabinets for event-

based data collection. The proposed methodology of the diagnostic tool is based on classical traffic engineering fundamentals and thus makes the results traceable and readily understood by the users. The implementation is demonstrated based on instrumented sites on TH 13, MN. Note that the diagnostic algorithms present in this chapter is intend for preliminary and quick evaluations regarding the offsets, splits and cycle lengths, while more detailed algorithms for offsets and splits fine-tuning will be present in the next.

CHAPTER 3
OFFSET EVALUATION AND FINE-TUNING

This chapter will introduce the evaluation and fine-tuning procedure for the offsets, with focus on constructing TS-Diagram to visualize progression quality for arterials. The proposed procedure is demonstrated with field cases and validations were performed using detector data and probe vehicle trajectories data collected from fields. An experiment is then carried out to illustrate how signal parameter changes could be made by intuitively evaluating the generated TS-Diagram.

3.1 Background about Time Space Diagram

Time space diagram (TS-Diagram) is a popular visualization tool for traffic signal evaluation, and has been used widely for signal operations (Koonce et al., 2008). With the time and distance as the X-Y axes, vehicle trajectories and signal status are commonly shown in a TS-Diagram. With the graphical illustration of the queues and delays, the progression quality can be evaluated intuitively. **Figure 3.1** plots one example of TS-Diagram, with trajectory of one vehicle and signal status at two intersections. Delay of the subject vehicle due to traffic signals can be clearly observed. If similar delays occur for the majority of the vehicles, a poor progression quality will be indicated.

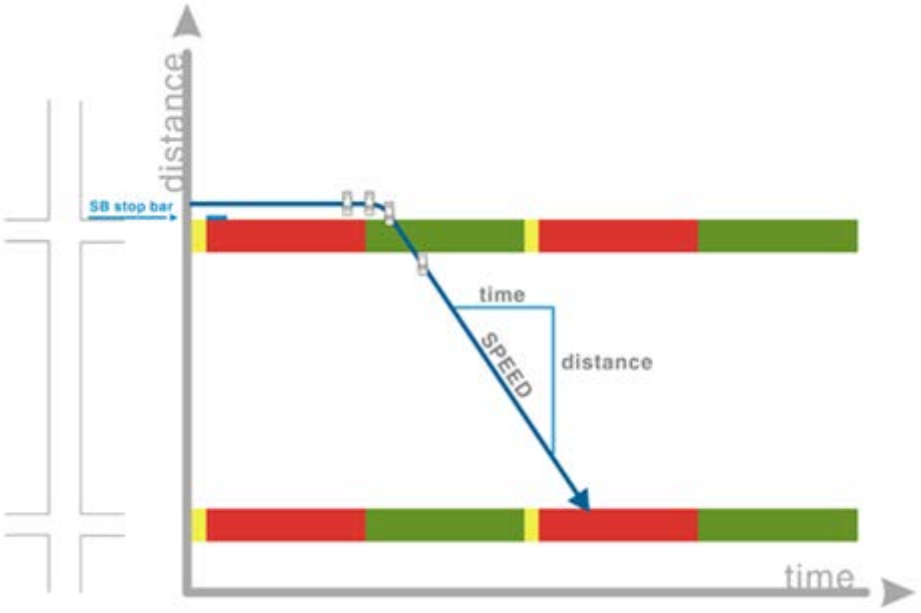

Figure 3.1 Example of TS-Diagram

[Source: Koonce et al., 2008]

Because of such convenience, TS-Diagram has been utilized by several commercial software as an output of signal optimization. For instance, TRANSYT-7F plots TS-Diagram with the green bands, and Synchro provides options to plot simulated trajectories in its TS-Diagram (Wallace et al., 1998; Husch & Albeck, 2006). A screenshot of Synchro TS-Diagram is illustrated in **Figure 3.2**, with blue and red lines as the trajectories of southbound and northbound traffic, respectively.

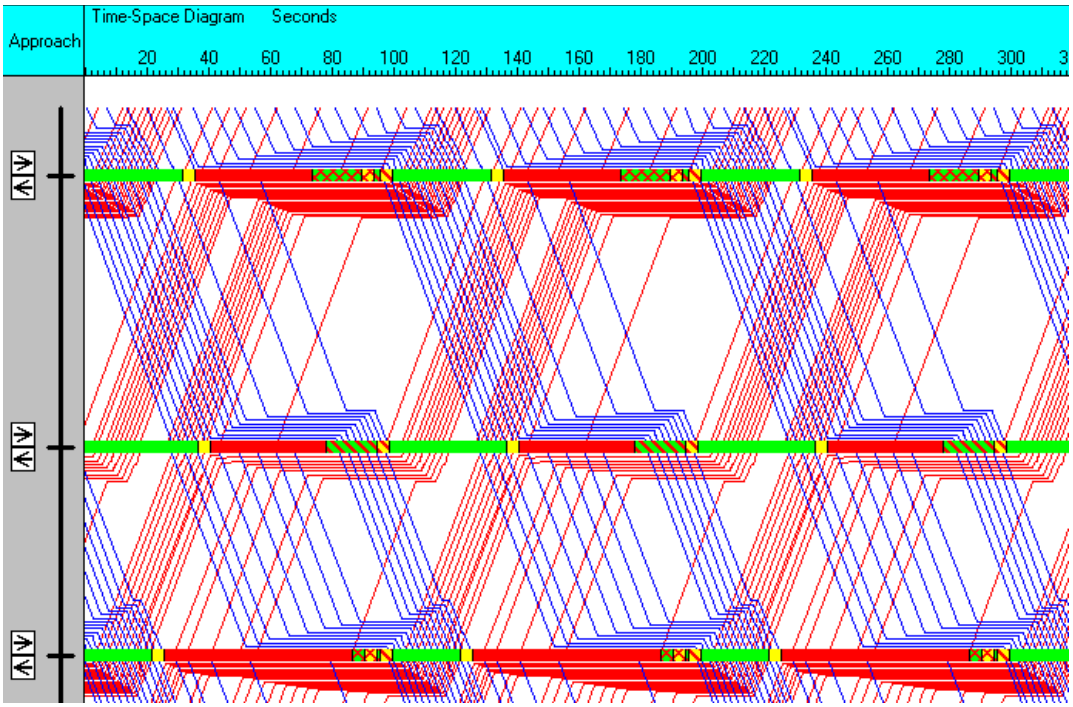

Figure 3.2 Screenshot of Synchro TS-Diagram

In the practice, the Synchro TS-Diagram is being used widely, to design or update signal timing parameters in the signal retiming process. An accurate Synchro TS-Diagram can properly reflect the field traffic condition, and help engineers choose appropriate timing parameters. On the contrary, inaccurate Synchro TS-Diagram, could mislead the engineers, degrade the timing performance, and increase the fine-tuning efforts. More importantly, since the Synchro TS-Diagram only uses manually collected data during a limited period, it cannot reflect the changing traffic conditions over time.

On the other hand, many intersections in the US are now using actuated signals, whereas few agencies have archived or analyzed the detector and signal status data to help signal operation (Liu et al., 2008). Recently, increasing attentions have been paid on using detector and signal data for performance evaluation and optimization of the traffic signal system. However, to the best of our knowledge, few studies have been done to generate the TS-Diagram for evaluation of signal coordination. This research attempts to fill in this gap.

In this chapter, we propose a practical procedure to generate TS-Diagram using the high-resolution event-based traffic data collected from the field. With data collected and archived automatically, the TS-diagram can be generated periodically without significant labor cost. This is particularly beneficial for the practitioners to evaluate traffic signal performance after the retiming process, or to fine-tune the system over time. The proposed procedure is demonstrated with field examples and validations were performed using detector and probe vehicle trajectories data. Then, an experiment is demonstrated to illustrate how signal parameter changes could be made by intuitively evaluating the generated TS-Diagram.

3.2 Constructing Link TS-Diagram

The proposed procedure is to first generate TS-Diagrams for each link individually. Then, the link TS-Diagrams are combined as the arterial TS-Diagram. Note that, for two opposite through

directions, there are two links between two adjacent intersections. The TS-Diagrams of these two links are overlapped, similarly to the Synchro TS-Diagram. Then the TS-Diagrams of consecutive links are stacked up sequentially, to form the arterial TS-Diagram.

In light of the cyclic nature of the traffic signal system (Day et al., 2010a), the TS-Diagram is constructed cyclically using data aggregated from multiple cycles. This indicates no variations of traffic patterns over different cycles in the plot. The reason is that traffic signal parameters are generally governed by dominant cyclical patterns while variations from cycle to cycle are usually limited with TOD operation. Moreover, the aggregation can help reduce the data noise from the detector, and make it easy to evaluate the average performance of a timing plan. Two steps are involved to generate a link TS-Diagram, described as follows.

Step 1. Aggregating high-resolution event-based data

In this step, both detector and signal data are aggregated. The detector event data is aggregated as the average cyclic flow profile (CFP), i.e. the interval volume over time within a cycle. Note that, the CFP has been used in TRANSYT-7F and SCOOT system (Wallace et al., 1998; Robertson & Bretherton, 1991), as well as some other researches for offset optimization (Abbas et al., 2001;Gettman et al., 2007; Day & Bullock, 2011). Here, we calculate the CFP of the through traffic at the link entrance, based on the advance detector data. To do so, the time instances of vehicle arrivals at the link entrance are estimated first. Depending on the queue impacts on the detector data, two cases need to be considered.

Case A: Queue does not propagate to the advance detectors

In this case, all vehicles would travel from the entrance to detector location in free flow speed. Hence, the arrival time at entrance are estimated by simply shifting the arrival time at the detector location with free flow travel time, as expressed by formula (3.1).

$$t_e(k) = t_d(k) - \frac{l_d}{v_f} \tag{3.1}$$

Where:

$t_e(k)$ is arrival time of k th detector actuation event at link entrance,

$t_d(k)$ is start time of k th detector actuation event at detector location and is measured directly,

l_d is distance from detector location to the link entrance, and

v_f is free flow speed.

Case B: Queue propagates to the advance detectors

In this case, vehicles may not all travel freely from the entrance to detector location, as some vehicles are delayed by the queue. Hence, the shifting in formula (3.1) is not applicable for all arrivals. Such cases can be identified with the queue over detector (QOD) phenomena from the detector data (Liu et al, 2009; Wu et al., 2010). This is illustrated in **Figure 3.3**. After the red starts, if a long queue exists, the detector will see vehicles standing at the detector location for unusually long time. The end time of this particular actuation event is when the vehicle on the detector starts to move after green starts, followed by queuing vehicles passing the detector at a saturated departure rate. In **Figure 3.3**, Point A indicates the time when queue propagates to the detector location. Point B indicates the time when the queuing vehicle on the detector starts to

move, and Point C indicates the time when the last queuing vehicle passes the detector. The arrivals between points A and C are delayed by the queue, and need further adjustment to estimate their arrival times at the entrance. The corresponding detector status is also shown in **Figure 3.3**.

To estimate the arrival time of the delayed vehicles, we adopt the algorithm in (Liu et al., 2009). Essentially, the algorithm attempts to identify three points A, B, and C based on the occupancy times and the time gaps from the vehicle-detector actuation event data. The points A and B can be identified as the start and the end of a detector event with long duration time. Point C, the end of queue departure, could be identified as the end of consecutive saturated departure events after green start, followed by a large gap. For more details of identifying point A, B, and C, we refer to (Liu et al., 2009). After the points A, B, C are identified, the arrivals are assumed as uniform arrivals between Point A and C, as expressed in the formula (3.2).

$$t_e(k) = \begin{cases} t_d(k_A) + \frac{(k-k_A)}{k_C-k_A}[t_d(k_C) - t_d(k_A)] - \frac{l_d}{v_f}, for\ k \in [k_A, k_C] \\ t_d(k) - \frac{l_d}{v_f}, Otherwise \end{cases} \quad (3.2)$$

Where:

k_A is index of detector event starts at Point A, and

k_C is index of detector event at Point C.

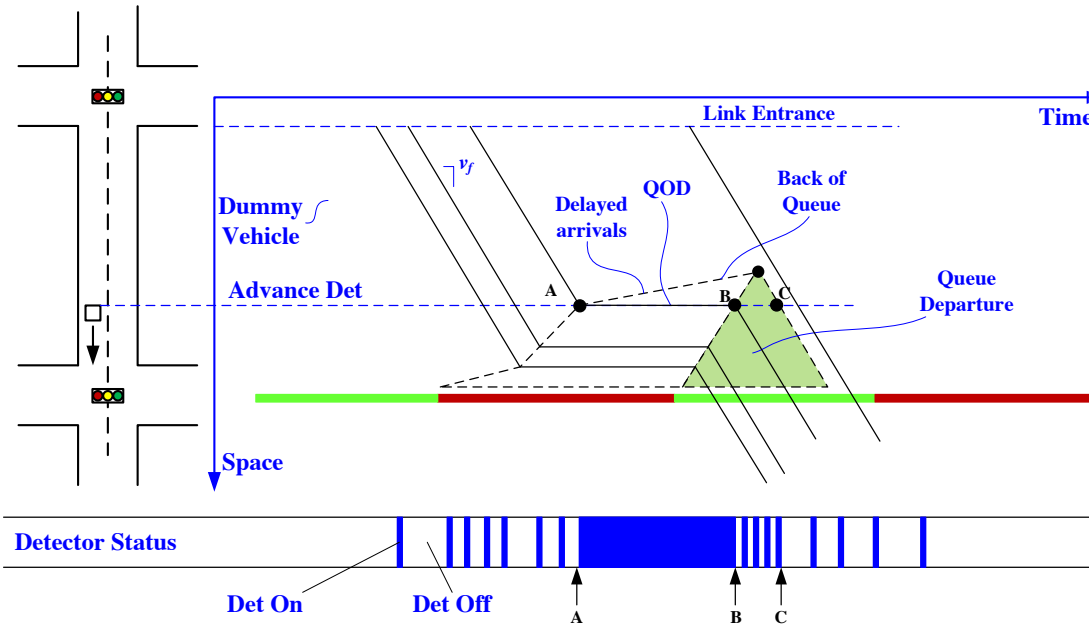

Figure 3.3 Illustration of queuing at intersection with QOD

Based on the estimated arrival times at the entrance, the interval volume can be then calculated using formula (3.3).

$$q(j) = \sum_{k=1}^{N} \mathbb{1}\{j\Delta t \le t_e(k) < (j+1)\Delta t\},\ for\ j = 1,2 \dots T. \quad (3.3)$$

Where:

$q(j)$ is volume of j th interval over investigation period,

Δt is the length of interval,

j is the index of interval over investigation period,

N is the total number of detector events,

T is the total length of investigation period, normalized by Δt, and

$\mathbb{1}\{.\}$ is the indicator function, with 1 if condition within bracket is satisfied, and 0 otherwise:

Then, the average CFP can be obtained by aggregating interval volume over cycles using formula (3.4). One example of the CFP with 5 sec interval is shown **Figure 3.4.**

$$\hat{q}(i) = \frac{\sum_{Mod(j,C)=i} q(j)}{N_c},\ for\ i = 1, \dots, C. \quad (3.4)$$

Where:

$\hat{q}(i)$ is flow of i th interval over time within cycle, as the CFP,

N_c is total number of cycles during investigation period,

C is for cycle length, which is the cycle length divided by Δt, and

Mod (,) is the modulo operator.

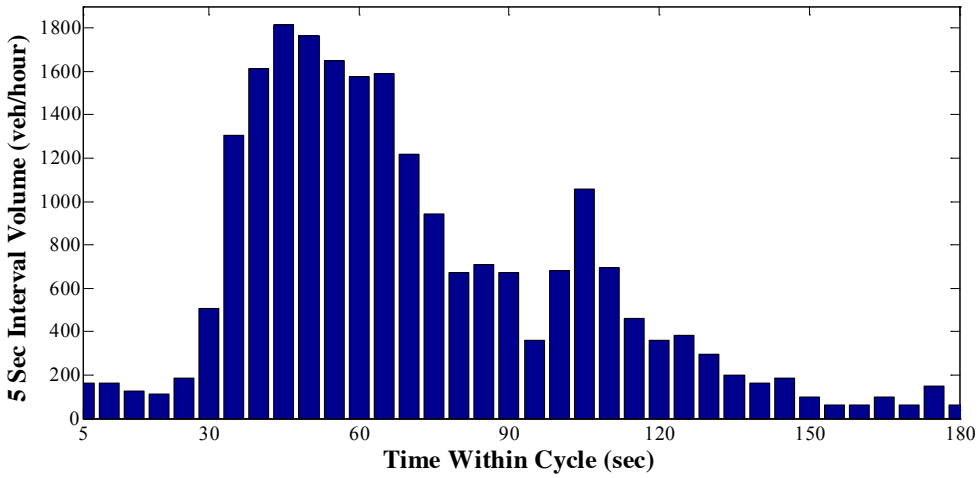

Figure 3.4 Example of CFP

Based on signal event data, the average green start and end of the associated phase are calculated by formula (3.5). For simplicity, yellow signal is treated as part of red signal.

$$\begin{cases} \bar{t}_{gSt} = \frac{\sum_{k=0}^{N_c} Mod(t_{gSt}(k),C)}{N_c} \\ \bar{t}_{gEd} = \frac{\sum_{k=0}^{N_c} Mod(t_{gEd}(k),C)}{N_c} \end{cases} \quad (3.5)$$

Where:

$\bar{t}_{gSt}$ is the average green start time over time of cycle,

$t_{gSt}(k)$ is the time of k th green start,

$\bar{t}_{gEd}$ is the average green end time over time of cycle,

$t_{gEd}(k)$ is time of k th green end, and

all variables including $\bar{t}_{gSt}$, $t_{gSt}(k)$, $\bar{t}_{gEd}$, $t_{gEd}(k)$ are normalized by Δt.

Step 2. Generating Virtual Trajectories

The CFP, average green start and end will be used to generate the link TS-Diagram. Before plotting, based on the CFP, a sequence of time instances at the link entrance will be generated, simulating virtual vehicles entering the link. This is a little tricky, due to the non-integer flow rate during an interval. For instance, with a 5 sec interval length, if a 1800 vehicle per hour (vph) flow rate is observed for the 1st interval, and 800 vph for the 2nd interval, , the problem is then to simulate 2.5 vehicles during 1st interval window, and 1.25 vehicles for the 2nd interval. One approach is to rounding up the numbers of vehicles, but it will introduce substantial rounding up errors. Instead, we simulate 250 vehicles equally spaced in the 1st interval, and 125 vehicles in the 2nd interval. Then, 100th, 200th, and 300th vehicles over the 10 sec horizon will be selected as the virtual arrivals to generate the trajectories. This approach can be viewed as generating fraction of vehicle based on flow rate. Then fractions are accumulated as whole vehicles.

At each time instance, a vehicle is simulated traversing from the entrance to stop bar, using the Newell's simplified car following model (Newell, 2002). In Newell's model, the follower's trajectory is simply a temporal-spatial translation of the leader in car-following mode. The calculation is expressed in formula (3.6).

$$x_i(t+\tau) = Min\{x_{i-1}(t) - d, x_i(t) + \tau v_f\} \quad (3.6)$$

Where:

$x_{i-1}(t), x_i(t)$ are the trajectories of the leader and follower respectively,

τ is the time displacement, and

d is the space displacement.

To account for the signal impact, a dummy vehicle based on red signal is generated as the first leading vehicle within the cycle. The procedure is repeated cycle by cycle to expand the plot. The illustration of the dummy vehicle is shown in **Figure 3.5.**

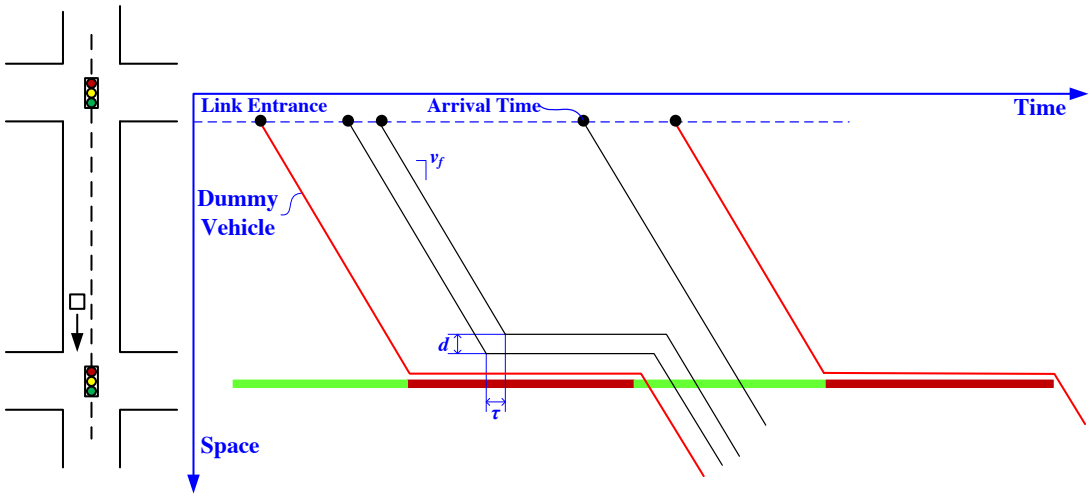

Figure 3.5 Illustration of car following and dummy vehicle.

3.3 Validation of TS-Diagram

Two cases are demonstrated, using data collected on Trunk Highway (TH) 55 and TH 13 in Minnesota. Both arterials are operated with vehicle-actuated coordinated control. Here, the parameters of the car following model are not calibrated but using typical values. In details, the post speed limit was used as the free flow speed, around 50 mph. 30 ft and 1.6 sec were used for the space and time displacement, approximately leading to jam density of 175 vehicle per mile (vpm) and capacity of 1800 vph.

3.3.1 Case 1: TH 55

Five intersections on TH 55 deployed with the SMART-Signal system are highlighted, with data collected on Nov 17th, 2008, from 7:15 AM-8:45 AM, when the morning peak timing plan was running. The TS-Diagram are shown in **Figure 3.6**, with arterial layout. In addition to the advance detectors, there were also temporary detectors at the link entrances for research purpose.

The eastbound (EB) and westbound (WB) trajectories are plotted with blue and red lines, respectively. The associated signal status for each direction was plotted facing the corresponding trajectories. As can be seen clearly, although the link TS-Diagrams were constructed independently, the traffic patterns were consistent across intersections, reflecting the consistent progression impact from the signal. This can also be viewed as a preliminary validation of traffic patterns in the TS-Diagram.

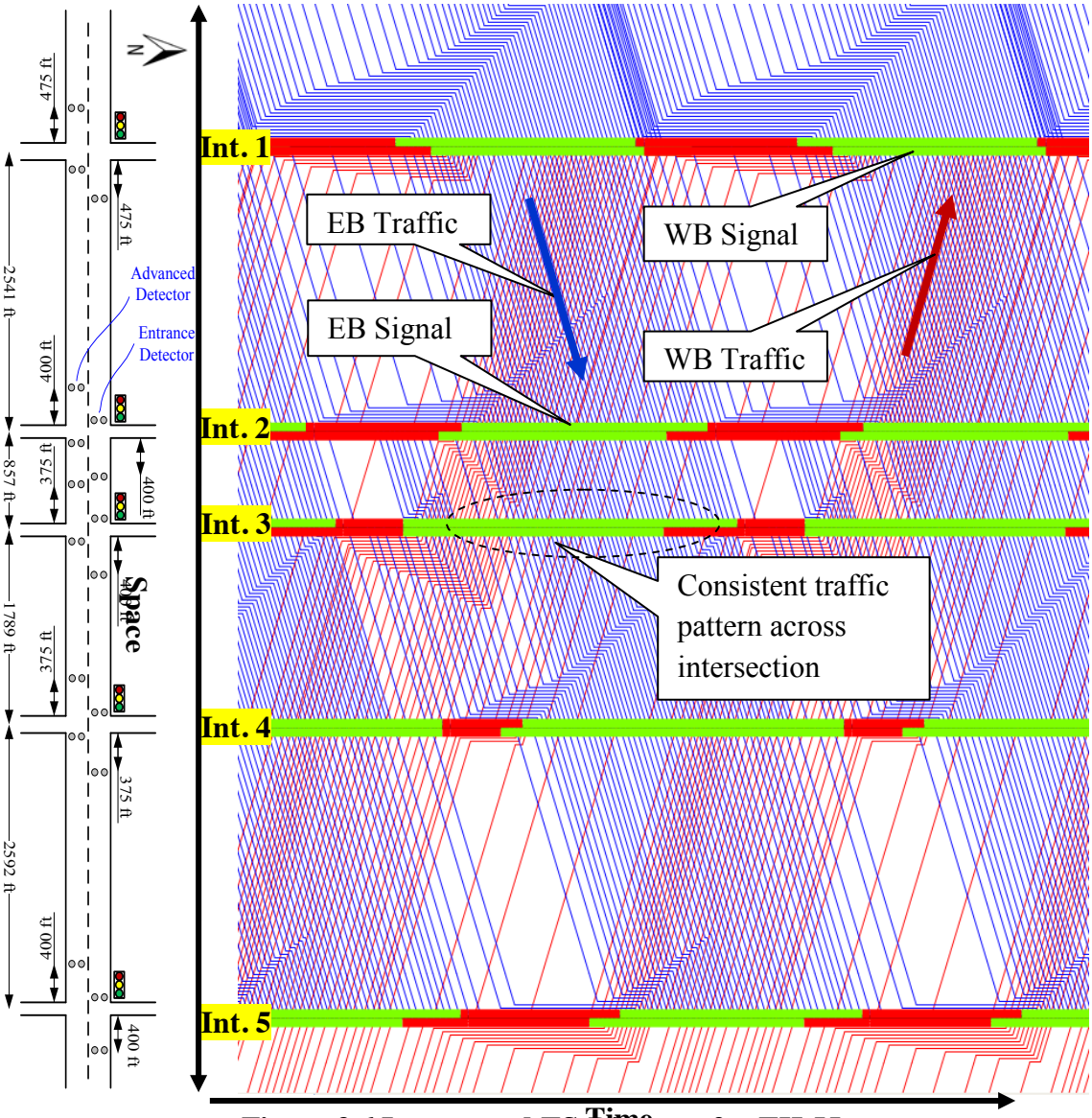

Figure 3.6 Layout and TS-Diagram for TH 55

Using data from the entrance detectors, a comparison was conducted, regarding the estimated and observed CFPs at the entrances. For each link, the total volumes from advance detectors and entrance detectors were balanced to reduce the impacts from the sinks and sources. The result is shown in **Figure 3.7**. As we can see, the estimated CFPs match well with the observed CFPs, indicating good estimation by the proposed method.

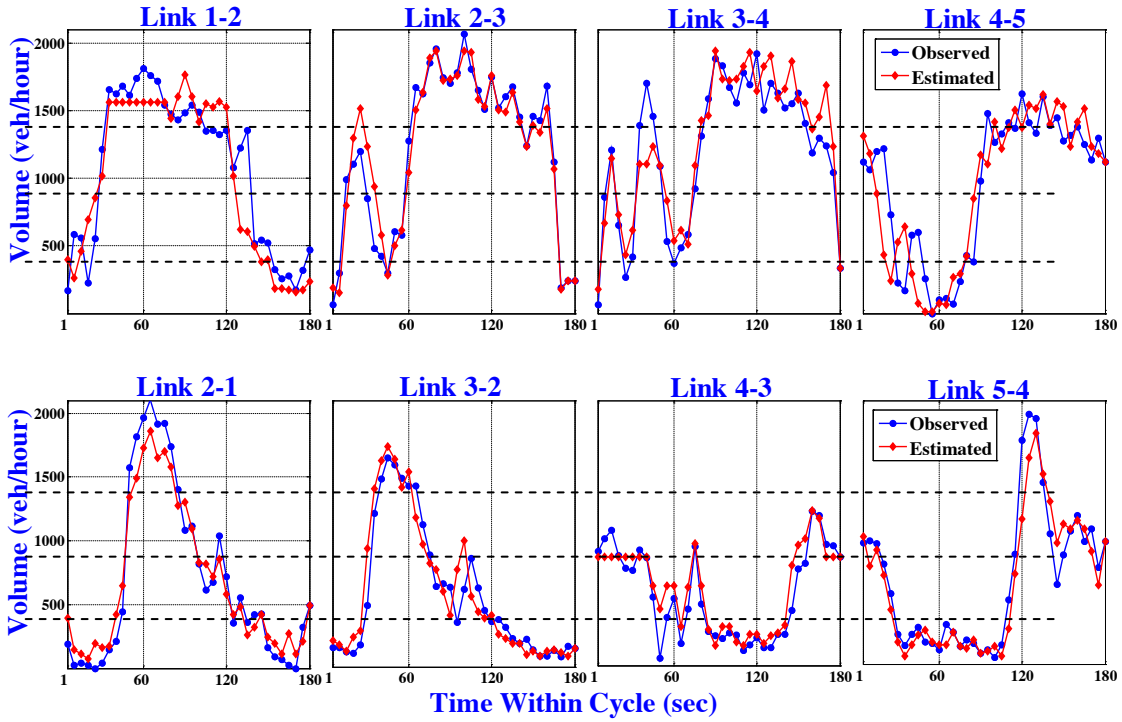

Figure 3.7 Estimated CFPs VS Observed CFPs for EB (Up) and WB (Down) traffic

3.3.2 Case 2: TH 13

In this case, seven intersections on TH13 with the SMART-Signal system were selected. The data was collected during afternoon peak period, from 4:30 to 6:00 PM, on Jul 23, 2013, with GPS data of nine field rides through the selected intersections. The TS-Diagram is shown in **Figure 3.8**, with the field ride trajectories in black. Note that, the field rides were actually made during several cycles, but were plotted within a single cycle based on individual departure time within each cycle at both ends of the arterial.

As indicated in the figure, the EB trajectories match well with the generated TS-Diagram, while some disagreements were found, indicated by letter A and B. This is expected as the TS-Diagram only reflects the average conditions, and cannot reflect the variations of the green start due to side street actuations and pedestrian calls. Similar disagreement was found for WB trajectories at Int. 6, denoted by C. However, significant disagreements were observed for WB trajectories approaching Int. 5, denoted by D. This was mainly due to the occurrence of WB oversaturation and residual queues at Int. 5. Due to the residual queues, the repetitive patterns were interrupted, resulting in amplified variations over cycles. This is evident from the significantly different trajectories traversing the intersection, while the vehicle entered the link at similar times within cycle. This indicates a limitation of the proposed TS-Diagram for the oversaturated intersections.

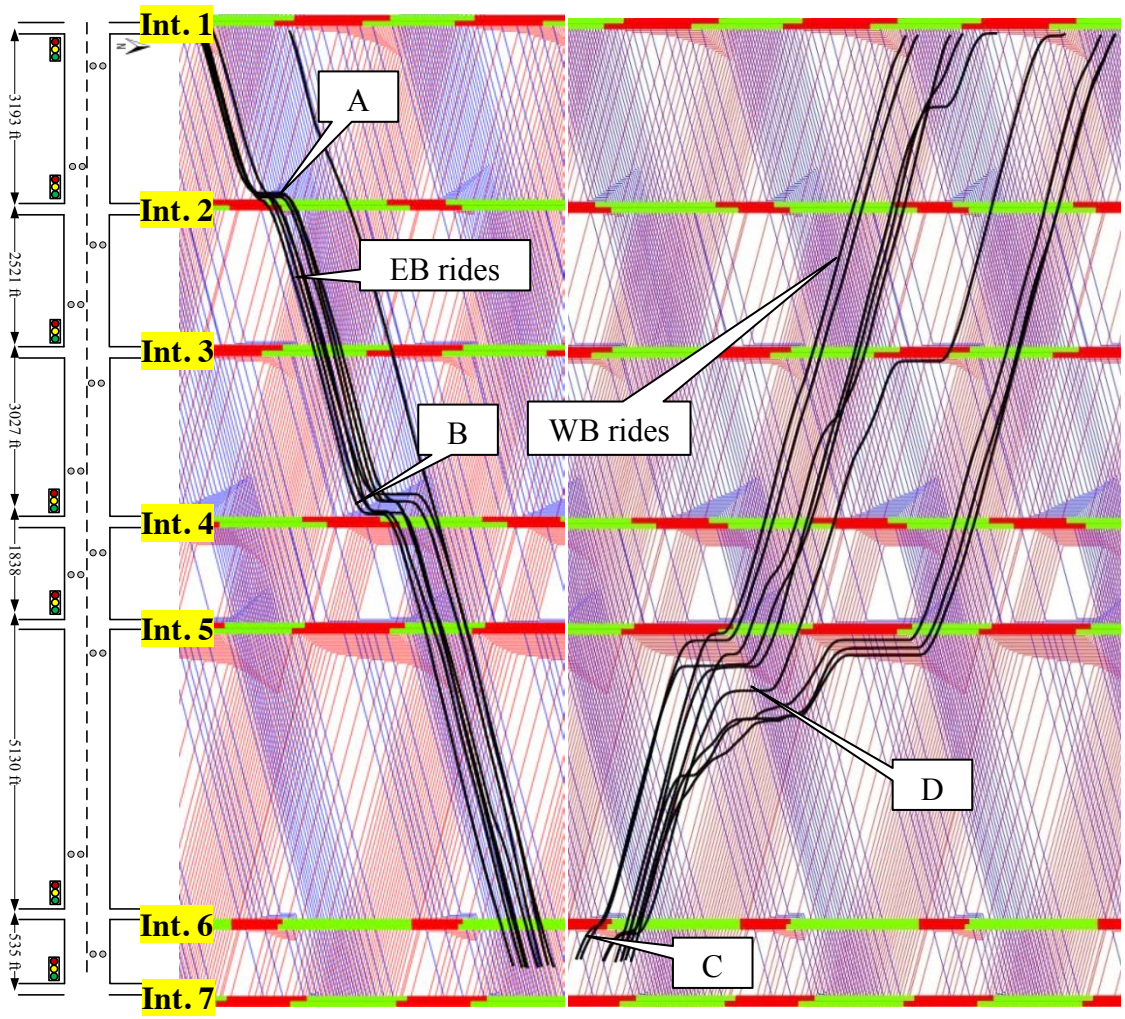

Figure 3.8 TS-Diagrams for selected intersections on TH 13

3.4 Fine-Tuning Using TS-Diagram with Offset and Lead-Lag Sequence

To illustrate the potential application of the TS-Diagram, an experiment was carried out to adjust the offsets and main street phase sequence, i.e. the lead-lag sequence, indicating whether the main street left turn phase is leading or lagging the through phase, for a eight-phase dual-ring NEMA controller. For the offset, we use green start of first coordinated phase as the reference point. Regarding the lead-lag sequence, there are four possible configurations for an eight-phase dual-ring NEMA controller, as shown in **Figure 3.9**. The configuration can be identified easily from the shape of overlapping green signals in the TS-Diagram.

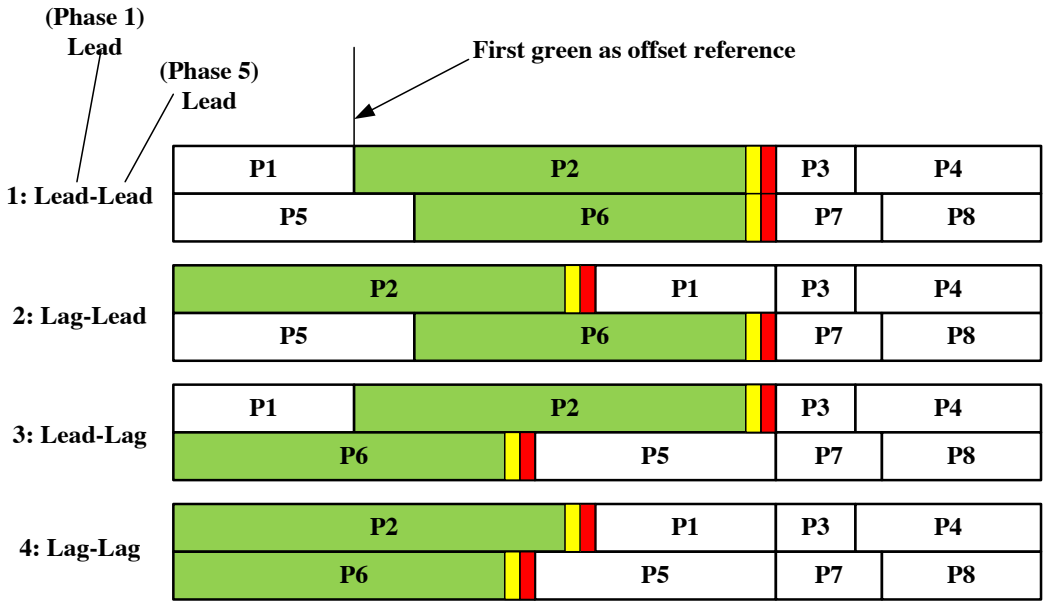

Figure 3.9 Offset reference point and combinations of lead lag sequence

So far, the TS-Diagrams are generated based on average data, reflecting the average traffic conditions. Many agencies, however, may concern about traffic signal performance for congested traffic conditions. To address such concerns, we also construct the TS-Diagram for relatively congested conditions, which will be the base of the analysis hereafter. To do so, when aggregating the raw data, the cycle volumes are calculated and ranked. Then, cycles with high cycle volume is kept and the rest will be filtered out. Here, we kept data with the highest 60-100 percentiles cycle volumes for each intersection, and constructed the TS-Diagram for the congested conditions. In practice, the criteria can be user specified, while our choice of 60-100 percentiles is to reflect relatively congested yet not extreme cases.

Both of the TS-Diagrams are shown in **Figure 3.10**, with Int.1 to Int. 5 of TH13 highlighted for analysis. The data was collected on four consecutive weekdays, 10/28/2013 to 10/31/2013, during 7:15 to 8:45 AM, for the evaluation of morning peak timing plan. Note that, while main traffic patterns remained similar, the queues were clearly longer in the congested case than the average case, indicated by letter A and B.

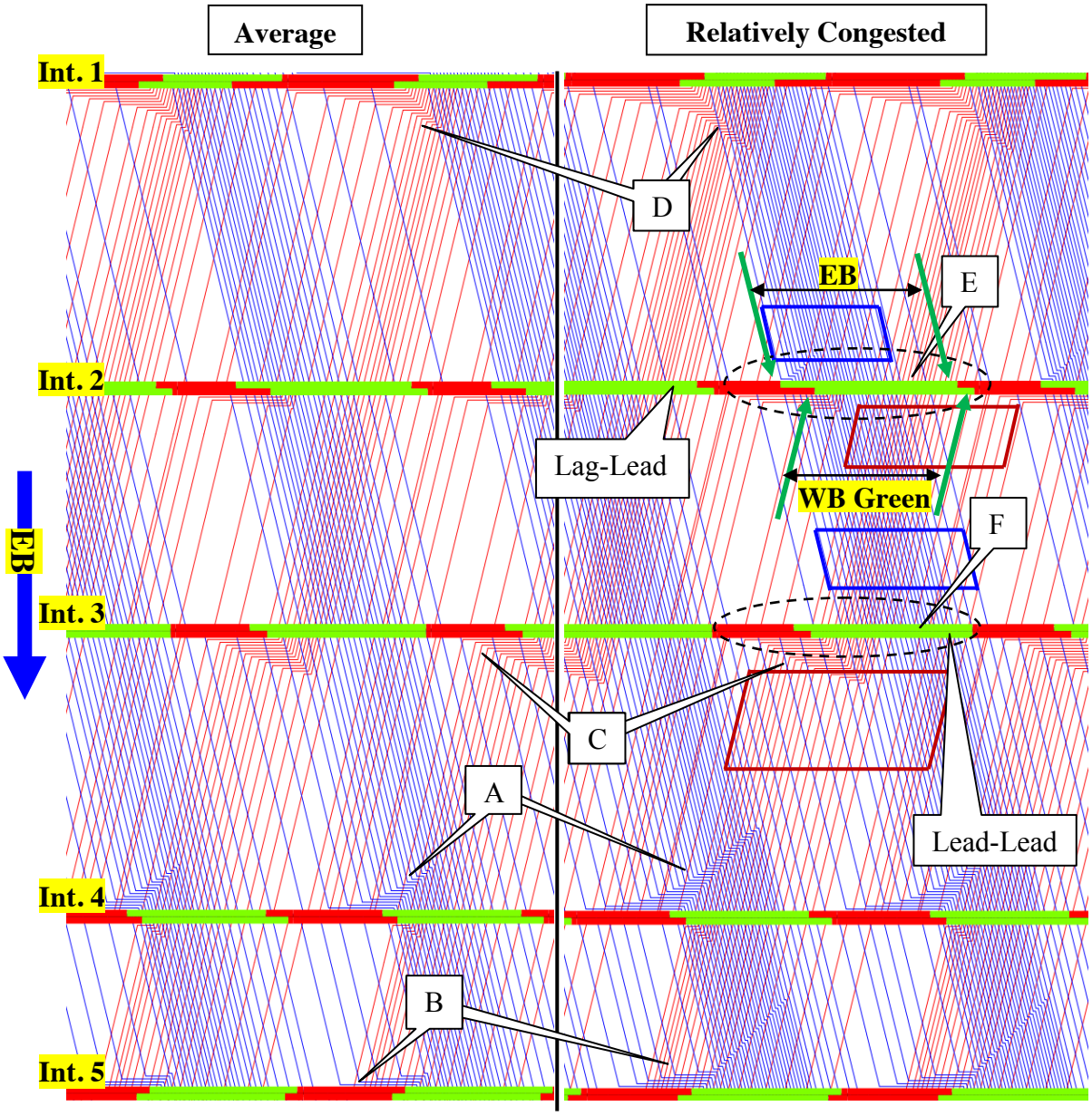

Figure 3.10 TS-Diagrams for selected intersections on TH 13 with average (left) and relatively congested conditions (right)

For a two-way coordinated arterial, trade-off exists for traffic in the opposite directions. With TS-Diagram, established method e.g. MAXBAND or combination method (Morgan & Little, 1964; Gartner & Little, 1975; Day & Bullock, 2011) can be incorporated easily for optimization. Here, instead of using a specific optimization method, we performed a quick, visual based evaluation of the TS-Diagram for the changes. Indeed, this would involve engineering judgment, and may lead to sub-optimal solution. For the sake of illustration, we will the visualization approach with this analysis, leaving systematic optimization for future research.

First, the queue length and delays were identified from the TS-Diagram. In **Figure 3.10**, the EB cases are indicated by letter A and B, with the WB cases by C and D. The offsets were

first fine-tuned for the direction with larger volume. The opposite direction was optimized next. Here, the EB was favored with a higher volume. The queues indicated by A and B, in the congested case, could be reduced by slightly shifting offsets to the left. The tradeoff exists with degraded WB performance at Int. 3 and Int. 4. This, however, should be minimal with the lower volumes. The decision was made to shift the offset at Int. 4 to the left for 4 sec, and 4 sec further to the left for offset at Int. 5, with a total 8 sec to the left at Int. 5. The 4 sec was selected arbitrarily because we want implement small adjustments only.

For the WB cases, to reduce the queue labeled with C, either the offset at Int. 3 needs to be shifted to the left, or offsets at Int. 4 and Int. 5 to the right. If offset at Int. 3 were shifted to the left, the end of EB platoon at Int.3 would be cut off and delayed by the red. If offsets at Int.4 and Int.5 were shifted to the right, the EB queues and delays would increase at Int. 4. Considering queue labeled with D, the end of the WB platoon was close to the green end, and would be delayed if offset were shifted to the left. Considering the overall benefit, no offset changes were justified regarding the WB cases.

Next, lead-lag sequences were evaluated. Here, we search for configuration of the lead-lag sequences that provides the max green window for the platoons in both directions. One example of a proper lead-lag sequence is indicated by E. The overlapping shape of platoon arrivals (EB first), indicated by the blue and red parallelograms was consistent with the overlapping shape of the green windows (EB first) for the two directions. This indicates the current setting of Lag (phase 1)-Lead (phase 5) was appropriate at Int.2. The intersections were evaluated one by one with similar logic. One potential change was identified, indicated by F. In this case, the end of EB platoon was cut off by the red signal, and could be better served by changing the Lead-Lead to Lead-Lag. The change was then granted. In addition, to accommodate the lead-lag change, the offset in Int. 3 was also shifted 7 sec to the left, so that there would not be unused EB green time after the end of EB platoon.

The offset and lead-lag changes are summarized in left part of **Figure 3.11**. For better illustration, the shifts of individual phases are indicated by the arrows. The changes were implemented from 11/05/2013 to 11/07/2013. Due to a connection issue, the data for 11/06/2013 was not available. The TS-Diagram generated using data collected on 11/05/2013 and 11/07/2013 is shown on the right part of **Figure 3.11**.

Slight changes of traffic patterns were found from **Figure 3.11**. For EB traffic, the shockwave at Int. 2, indicated by A, was slightly reduced. The EB arrivals near the start of red at Int.3 was better accommodated, indicated by B. No obvious change was found for the EB arrivals at Int.4, indicated by C. This is intriguing given the relatively large shift of EB phase at Int. 3. If observed carefully, the density of the lines for the arrivals has changed slightly as circled by the blue parallelograms, and both arrivals showed slight inconsistency with departures at Int. 3. The potential interpretation is as follows: in the before case, the drivers decelerated with anticipation of the queue formation, and the queuing profile at Int. 4 were based on the delayed arrival time, and were underestimated. For WB traffic, degraded performance was found at Int.1, Int.3 and Int.4. Some improvements were found at Int. 2, labeled by E, likely because main street arrivals near the green start and arrivals from the site street at Int. 3 were better coordinated.

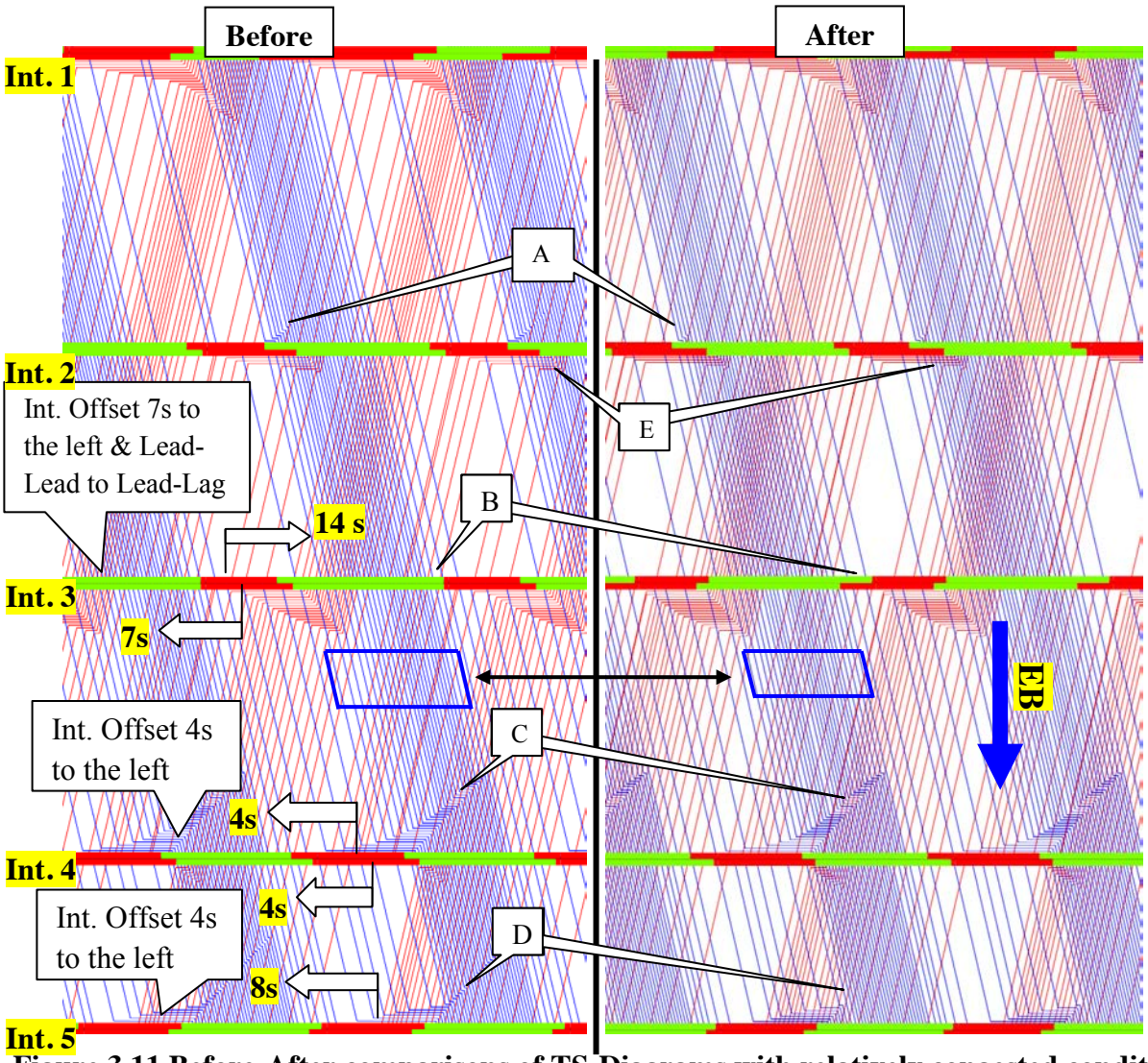

Figure 3.11 Before-After comparisons of TS-Diagrams with relatively congested condition

For further validation, the queue length and delay were estimated by the SMART-Signal system (Liu & Ma, 2009; Liu et al., 2009; Wu et al., 2010), and the results are summarized in **Figure 3.12** and **Table 3.1**. As indicated in **Figure 3.12**, average maximum queues were reduced for most of EB phases, while slightly increased for the WB phases. This is consistent with the TS-Diagram, as the proposed changes favored EB over WB traffic.

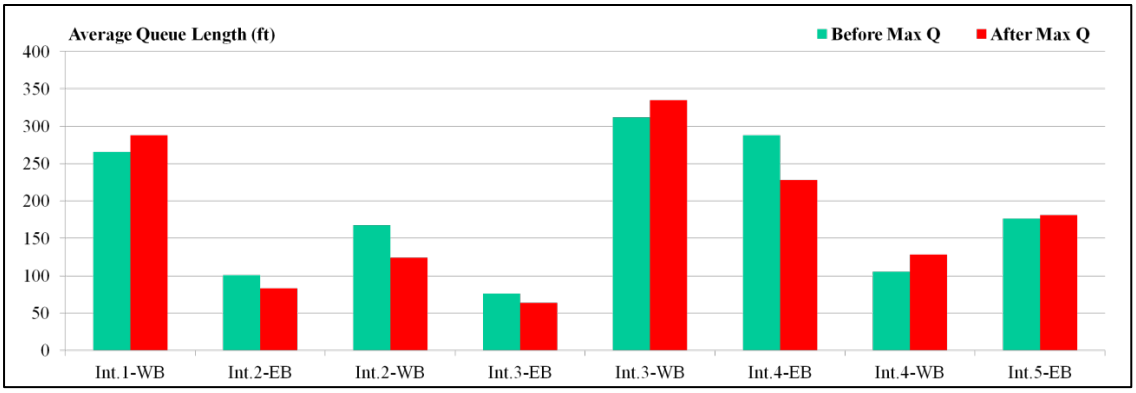

Figure 3.12 Before-After comparison of maximum queue length from SMART-Signal System

As indicated in **Table 3.1**, the average delay for EB travel was reduced by 14%, with 4.6 sec/veh, while for WB traffic, it increased by 4%, with 2.7 sec/veh. Overall, with the higher volume of EB traffic, the total delay was reduced by 4%, i.e., 163.8 veh sec/cycle.

Table 3.1 Before-After comparison of delay from SMART-Signal System

Average	Before	After	Abs. Change	Per. Change
EB Vol. (vph)	1314	1310	-4	0%
EB Delay (sec)	32.4	27.8	-4.6	-14%
WB Vol. (vph)	1003	1007	4	0%
WB Delay (sec)	65.3	68	2.7	4%
Cycle Delay (Veh*Sec)	4607.6	4443.8	-163.8	-4%

3.5 Conclusions

In this chapter, we proposed a practical procedure to construct the TS-Diagram for progression visualization of signalized arterials. The TS-Diagram can be constructed periodically based on high-resolution event-based traffic data that can be collected automatically and continuously. The field examples with validation were illustrated for the proposed procedure. Reasonable agreements were found based on entrance detectors data and field ride trajectories. A field experiment was carried out to illustrate the potential application of TS-Diagram, with focus on fining-tuning offsets and lead-lag sequence. Based on visual evaluation of the TS-Diagram, changes were recommended, and 4% reduction of total delays was achieved.

CHAPTER 4
GREEN SPLITS EVALUATION AND FINE-TUNING

This chapter will introduce the performance evaluation and fine-tuning module for the green splits.

4.1 Measure of Effectiveness for Green Splits

Assigning green splits proportionally to traffic demands is a simple while effective rule to determine green splits. To evaluate the performance of green splits, classical measures of effectiveness (MOE), the volume/capacity ratio (v/c ratio) is commonly used when designing signal timing parameters. However, in the conventional practice, the v/c ratios are only calculated during signal retiming process with manual collected data, and are not monitored continuously. Although the practice is limited, there are some researches trying to calculate v/c ratios using the detector and signal data for evaluation of the green split and cycle length (Balke & Herrick, 2004; Balke et al., 2005; Smaglig et al., 2007; Day et al., 2010a; Sunkari et al., 2011).

The green splits fine-tuning module proposed here can be viewed as an extension from (Smaglig et al., 2007; Day et al., 2010a). The main difference is, instead of using detector volume directly, we proposed a new MOE, the Utilized Green Time (UGT), extended from the queue service time (QST) for green split evaluation. The purpose is to address the issue that volume measured at stop bar detectors could be inaccurate, since the stop bar detectors are mainly for vehicle presence detection, especially when long or sequential detectors are used (Lawrence et al., 2006).

4.1.1 V/C Ratio

The v/c ratio indicates saturation level of a specified signal phase (TRB, 2000), and can be calculated cycle-by-cycle, as:

$$X_i(j) = \frac{V_i(j)}{s_i x_i(j)} \tag{4.1}$$

Where:

$X_i(j)$ is the v/c ratio of phase i, for j th cycle,

$V_i(j)$ is the flow rate of phase i, for j th cycle,

s_i is saturation flow rate of phase i,

$x_i(j) = \frac{g_i(j)}{C}$ is the green split, and,

$g_i(j)$ is the green time.

When long or sequential detectors are used, vehicle counts could be inaccurate. This is because consecutive arrivals may only cause a single detector actuation event with long duration length. One example from a sequentially connected detector at stop bar is shown in **Figure 4.1**, with example of detector actuation events. In such cases, occupancy-based measures will be more desirable.

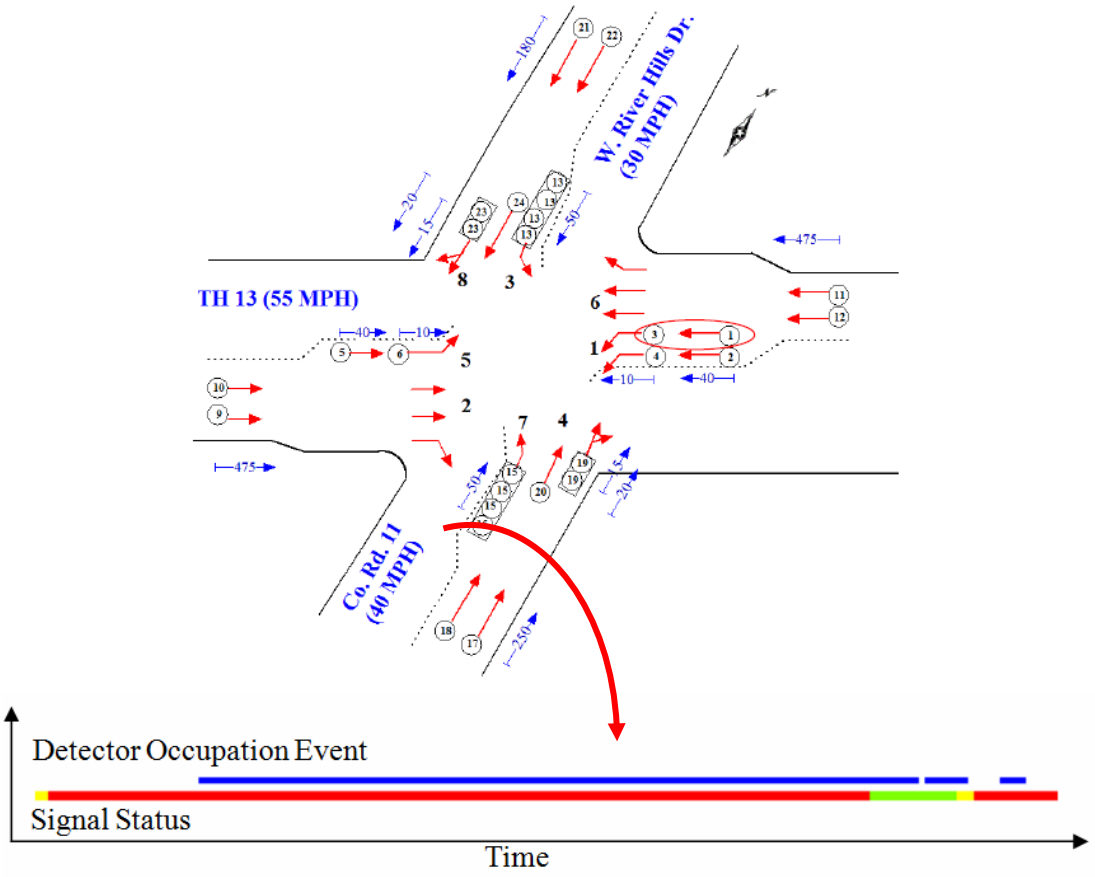

Figure 4.1 Example of traffic events from long detector at stop bar

4.1.2 Queue Service Time (QST)

Another important MOE is the Queue Service Time, defined as the length of green time used to clear the queue (TRB, 2000; Balke & Herrick, 2004). Balke & Herrick (2004) proposes to use the time elapsed from the green start to the start of first time gap identified from stop bar detector data, as the QST. This is based on the assumption that queuing vehicles will constantly place calls on stop bar detector until queue is cleared, which may not be the case if the detector is not long enough. Alternatively, we propose following formula for QST calculation. The key is to identify the end of queue departures, by detecting the first large gap from detector events. Here, a threshold gap value of 2.5 sec is used. An illustration of QST is shown in **Figure 4.2.**

$$QST_i(j) = t_{Q,i}(j) - t_{Gr,i}\ (j) \qquad (4.2)$$

Where:

$QST_i(j)$ is the queue service time for phase i, for j th cycle.

$t_{Q,i}(j)$ is the end of queue departure, and is identified as the start of the first gap larger than 2.5 sec after green start, and

$t_{Gr,i}(j)$ is the start of green.

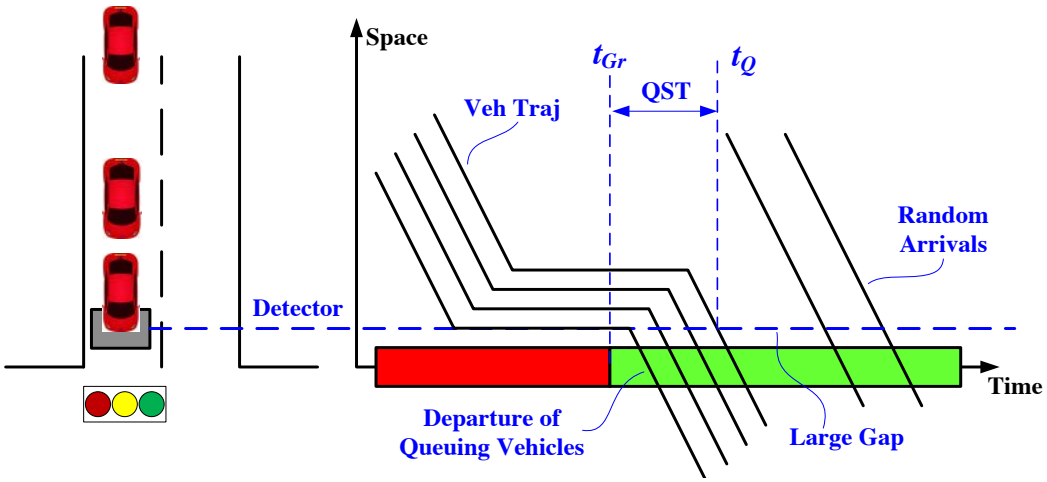

Figure 4.2 Illustration of QST

4.1.3 Utilized Green Time and Slack Green

While QST represents green time to clear the queue, it does not account for green time used by the vehicles that are not queuing. Based on the QST, the following formula is proposed to calculate the Utilized Green Time (UGT), as the total green time needed to serve the demand within a cycle. In the formula, the first part is the QST, while the second part represents the minimum green time needed to serve the rest of arrivals.

$$UGT_i(j) = QST_i(j) + h_{s,i} \times n_i(j) \quad (4.3)$$

Where:

$UGT_i(j)$ is utilized green time at phase i, for jth cycle,

$h_{s,i}$ is the saturation headway for phase i (2 sec in our study), and

$n_i(j)$ is number of random arrivals within green time after queue is cleared, at phase i, for j th cycle.

An example of calculation of QST and UGT is shown in **Figure 4.3**. As indicated in the figure, the green start is indicated as t_A, and the end of queue departure is indicated as t_B, followed by a relatively large gap with four additional arrivals. Hence, the QST is $(t_B - t_A)$, while the UGT is $(t_B - t_A + 4 \times 2\ sec)$.

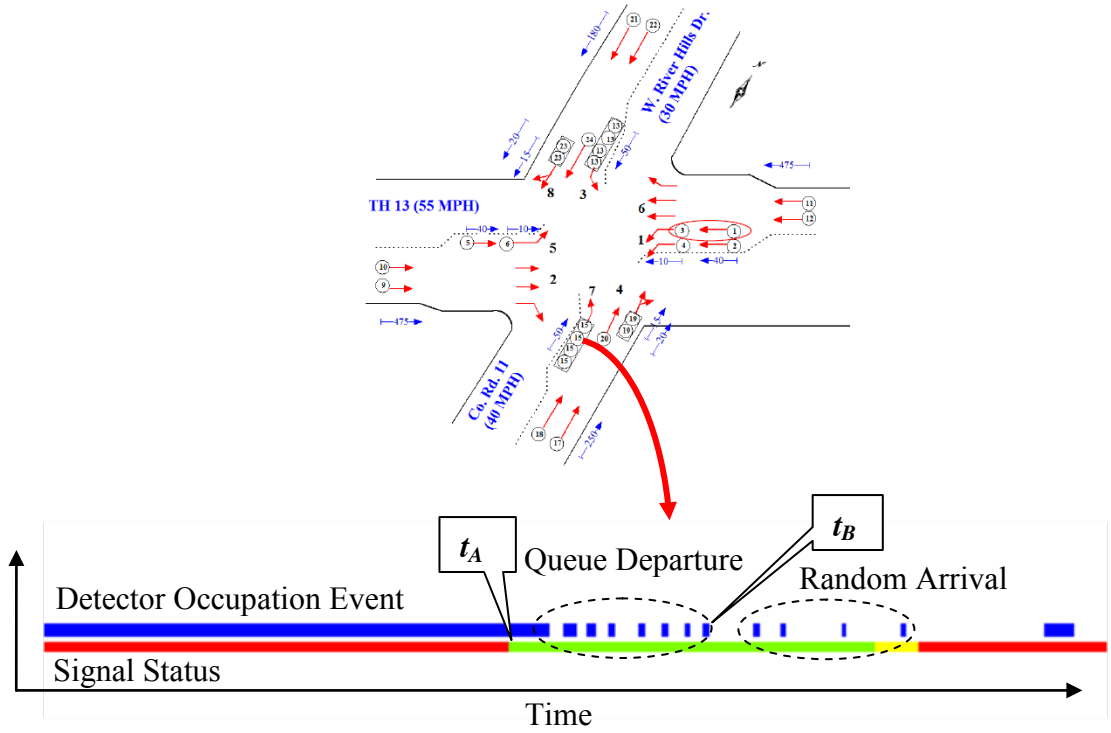

Figure 4.3 Example of QST and UGT calculation

Then, the slack green, $g_{Sl,i}$, unutilized to serve the traffic, can be calculated as:

$$g_{Sl,i} = g_i - UGT_i \tag{4.4}$$

Based on the slack green, the *phase failure* can be identified for cycles without any slack green, meaning that the green time may not be sufficient to serve all the demands within one cycle.

4.2 Green splits rebalancing based on UGT

For vehicle-actuated signals, traffic engineers are typically concerned with phase failures for non-coordinated phases. Therefore, the recommended fine-tuning rule is to maintain acceptable slack green time for each phase to reduce the potential phase failures (Day et al., 2010a). In addition, since the progression quality of coordinated phases is another major concern, the green split rebalancing is restricted to non-coordinated phases only.

In addition, since NEMA controller operates the two rings concurrently, in order to compare the phase utilization across different phases, the critical phases need to be identified first. The critical phases are phases with higher green utilization, hence, smaller slack green, than the concurrent phases on the other ring. General speaking, these are relatively more congested phases. For a typical eight phase NEMA dual ring controller, following rules can be used to identify the critical phases based on the slack green, excluding the coordinated phases.

- For phase 1, 5, if $g_{sl,1} < g_{sl,5}$, phase 1 is critical phase. Otherwise, phase 5 is critical phase.
- For phase 3, 4, 7, 8, if $g_{sl,3} + g_{sl,4} < g_{sl,7} + g_{sl,8}$, then phase 3 and 4 are critical phases.

Otherwise, phase 7 and phase 8 are critical phases.

Once the critical phases are identified, the splits can be first rebalanced across the critical phases. Since more slack greens exist at non-critical phases, further balancing across non-critical phases can be easily done to accommodate the changes at critical phases.

4.3 Split Fine-tuning Example

To demonstrate the split fine-tuning, an example is illustrated based on one of the intersections on TH13. **Figure 4.4** shows the layout of the selected intersection, at Nicollet Ave & Highway 13, Burnsville. The ring-and-barrier diagram is also shown in the figure. Six phases are used with a cycle length of 130 seconds, with phase 2 and 6 as coordinated phases, and the rest phases, phase 1, 3, 4, 5, non-coordinated. The numbers on the green bars in the ring-and-barrier diagram show the max green time, plus yellow and red clearance time. The detector and signal data used were collected during 1:30 pm to 3:00 pm, from 7/08/2013 to 7/12/2013, Mon to Fri.

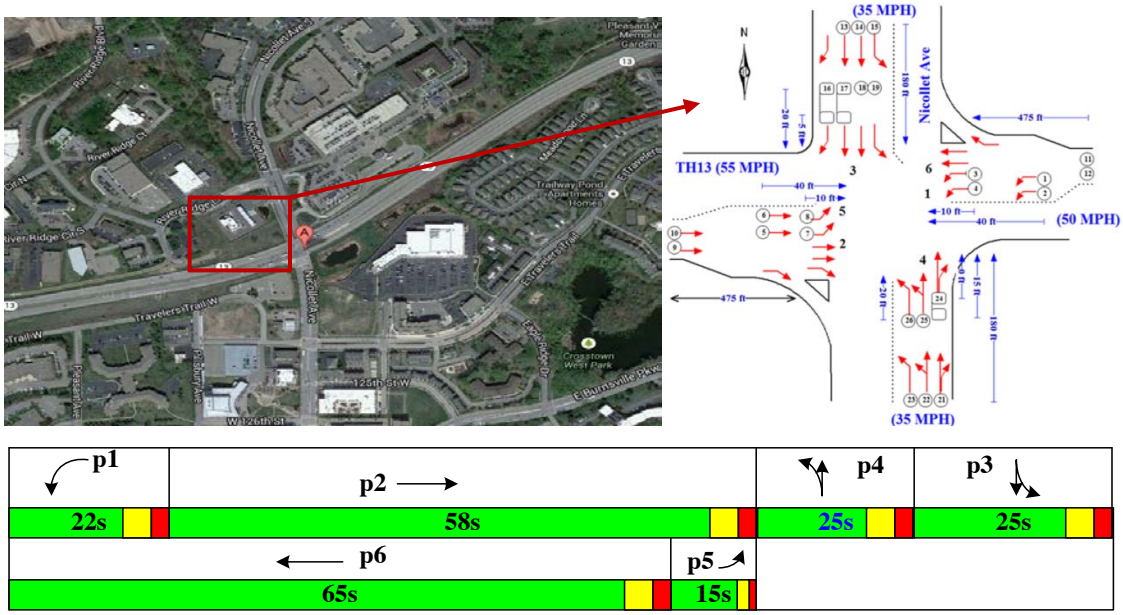

Figure 4.4 Intersection layout and ring-and-barrier diagram of the signal timing

In **Figure 4.5**, cycle-by-cycle green time with UGTs was plotted for the non-coordinated phases. The X-axis denotes the cycle index, while the Y-axis shows the length of time duration. The purple lines indicate the separation between two consecutive days. From the figure, varying green time was clearly shown at phase 1, 3, 4. Due to the fixed force off setting at coordinated phase 6, phase 5 was essentially operated as fixed-time. For phase 4 and phase 5, relatively high proportion of green has been utilized, with small slack green left, indicated by letter A. For phase 1 and phase 3, on the contrary, relatively large slack green was observed, indicated by letter B. This indicated opportunities to rebalance the green splits among the four.

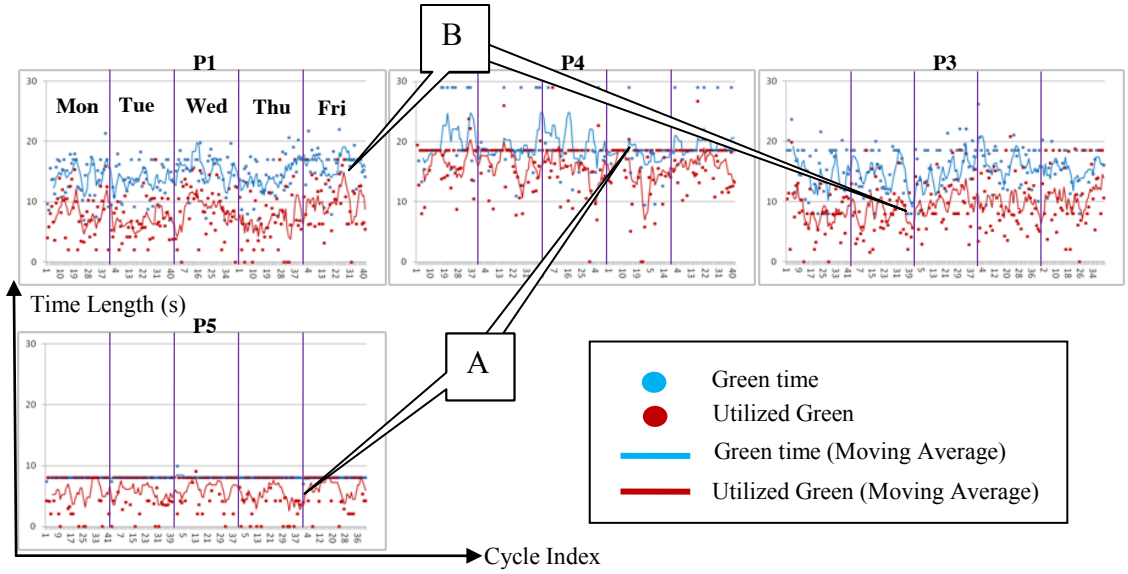

Figure 4.5 Green Time VS Utilized Green Time

After the aggregation of 5 days data, average statistics were summarized in the table in **Figure 4.6**. The information was further tabulated within the ring-and-barrier diagrams, for more intuitive interpretation. In the ring-and-barrier diagram, the green bar indicates the average green time, while the blue bar indicates the average UGT. For brevity, the yellow and red clearance signals were not plotted. The values of the UGT and green time were also denoted nearby the diagram, and were stated in the format as "Phase ID-UGT/Average Green, (Phase Failure rate)". For instance, "P3-9/15 (19%)", represents for "Phase 3 with 9 sec UGT, 15 sec Average Green, and a 19% phase failure rate".

Then, the critical phases were identified. The slack green at phase 5 was 2 sec, which was shorter than slack green at phase 1; hence, the phase 5 was the critical phase. Since no phase 7 and 8 were used, phase 4 and phase 3 were critical phases. Among the critical phases 5, 4 and 3, it would be feasible to reduce max green time for phase 3 slightly, with increase at phase 4 and 5, particularly when considering the relatively high phase failure rate with 57% and 36% at phase 5 and 4 respectively.

Table 4.1 Average Values for the MOEs

Phase ID	Max Green (s)	Average Green (s)	UGT (s)	Slack Green (s)	Phase Failure Rate[2]
1	17	15	8	7	3%
5[1]	10	8.0	6	2	57%
4	18.5	19	14	5	36%
3	18.5	15	9	6	19%

1: underline indicates this is a critical phase;

2: phase failure rate is the proportion of cycles with phase failures.

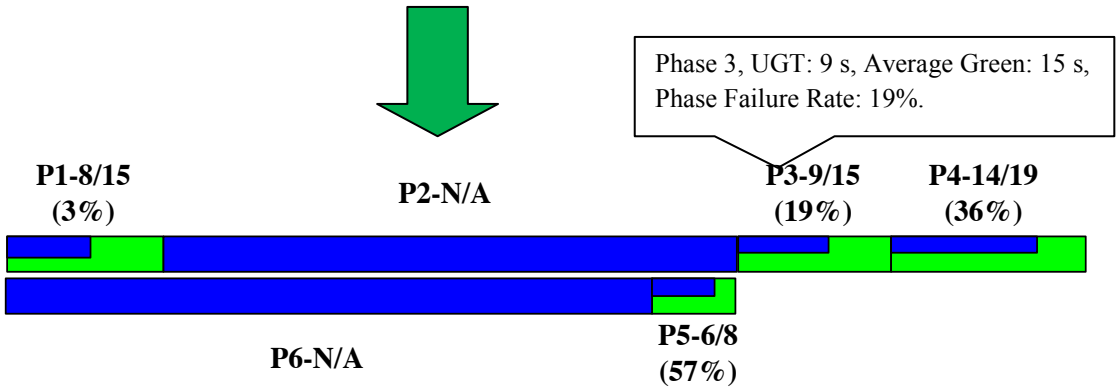

Figure 4.6 Ring-and-barrier diagrams with UGTs

4.4 Conclusions

In this chapter, we propose a new MOE, the UGT for green splits evaluation, based on queue service time. The proposed calculation of UGT explicitly considers the queuing process for better estimation of queue service time. The calculated statistics can be easily tabulated within the Ring-and-barrier diagram, to facilitate visual evaluation. The calculation is illustrated by an example using field collected data.

CHAPTER 5
OPTIMIZING AND FINE-TUNING TIME OF DAY TRANSITIONS

In this chapter, we will introduce the optimization and fine-tuning algorithm for Time of Day transitions among different timing plans for coordinated arterials.

5.1 Introduction

Urban traffic typically possesses time-dependent patterns over time of day, e.g. peak hour pattern and non-peak hour pattern. To accommodate these traffic patterns, traffic signal system commonly implements different timing plans over time of day (TOD), which is the TOD operation. In the current practice of signal operation, due to the lack of convenient, easy-to-use optimization tools, transitions between different timing plans, or TOD transitions for short, are largely determined based on engineering judgments. It may thereby lead to an inefficient operation of traffic signals systems. To reduce such deficiencies, we aim at developing an easy-to-use, while theoretically sound, approach to assist traffic engineers to determine proper TOD transitions using detector and signal status data for signalized arterials.

Even though it is limited in practice, several researches so far have proposed methodologies aiming at systematically optimizing TOD transitions. Among work been reported, statistical clustering approach has been a popular choice to identify proper TOD break points. The essence is to group time periods into different clusters based on specific measures. Smith et al (2001) deployed a hierarchical statistical cluster approach to determine TOD points. In their work, TOD candidates were eliminated based on Euclidian distance using state vectors of volumes and occupancies. In Wang et al. (2005), a non-hierarchical clustering, the K-Mean clustering is used. The main difference with the hierarchical clustering method is the simpler calculation. However, the algorithms in both work may generate unreasonable clusters, the outliners (Park et al., 2004), that will lead to unrealistic, frequent transitions. And subjective interventions are required before implementation. To reduce outliners, more recently, Ratrout (2010) proposed to use Z-Score of the volume in lieu with time, to construct state vector for clustering. Commercial software i.e. SYNCHRO and SimTraffic were then integrated into the proposed procedure for optimization.

Instead of using statistical approach, other researches focus on refining TOD transitions based on performance measures such as delay or stops, assuming that initial TOD break points are given. In this way, signal performance could be considered more explicitly. For instance, Park et al. (2004) proposed a two-stage optimization procedure using genetic algorithm (GA) to determine optimal TOD breakpoints. The inner loop optimizes splits and cycle length based on delay formula from HCM (TRB, 2000), while the outer loop refines the TOD break points to minimize total delay. However, neither the coordination impact nor transition cost was taken into account. Later, Park & Lee (2008) proposed a procedure utilizing micro-simulation to determine optimal TOD break points. Initial breakpoints are determined by visually inspecting optimal cycle length first, and are then refined based on performance measure calculated by a micro-simulation software e.g. CORSIM. In Abbas & Sharma, (2005), a multi-objective evolutionary algorithm based approach is proposed to optimize TOD break points. They proposed the degree of detachment (DOD) as a performance measure for transition frequency of signal plans. The DOD, together with delay and stop, is then used to determine Pareto optimality regarding TOD

transitions. Signal optimization software, PASSER V, was used to generate optimal signal timing parameters within each period, as well as calculating delay and stops.

From pervious researches, several shortcomings can be summarized. Some approaches, e.g. Smith et al. (2002) and Park et al (2004) do not take into account coordination quality of signal plan, but only concentrate on performance at individual intersections. Other researches rely on micro-simulation to calculate performance measure. To properly set up such evaluation, substantial efforts e.g. calibration, are incurred and accuracy may vary on a case-by-case basis. Moreover, the majorities of these approaches are aiming at design stage of signal timing, and may not be appropriate in cases when only some refinements are desirable after the signal retiming.

In this chapter, we propose an easy-to-use approach to fine-tune TOD transition, by revisiting the approaches proposed in Park et al. (2004) and Park & Lee, (2008). Different from previous methods with focus on the design stage of signal timing, the scope of the proposed procedure is restricted to refining TOD transitions, assuming that signal plan parameters are given and remain unchanged. Moreover, we assume that initial TOD transitions are available as well. For delay calculation, instead of using micro-simulation, we use HCM formula with explicit consideration of coordination quality. To estimate green duration of actuated traffic signals for delay calculation, a signal estimation model is proposed and validated using field collected data. The proposed approach could be particularly beneficial for practitioners to fine-tune TOD transitions for signalized arterials in the parameter fine-tuning process during signal retiming.

5.2 Methodology

Considering two timing plans at two joint TOD periods, our objective here is to determine an appropriate transition point between the two. If transition between two plans can be determined, the procedure can be similarly applied to determine transitions of several timing plans over the entire day. To determine such transition, here, the focus is on calculating performance measure for the candidate timing plans. As a popular choice, the total delay, which includes delays at all associated intersections, is selected as the performance measure. For coordinated arterials, the total delay can be further grouped as delays at coordinated phases and delays at non-coordinated phases, as expressed in Eq. (5. 1).

$$D(t, \boldsymbol{S_k}) = \sum_{[i,j]\in\emptyset_{nc}} {D_{nc}}^{[i,j]}(t, \boldsymbol{S_k}) + \sum_{[i,j]\in\emptyset_c} D_c^{[i,j]}(t, \boldsymbol{S_k}) \quad (5.1)$$

Where:

$D(t, \boldsymbol{S_k})$ is the total delay at time t, depending on k th candidate signal timing $\boldsymbol{S_k}$,

${D_{nc}}^{[i,j]}(t, \boldsymbol{S_k})$ is the delay for the lane with a non coordinated phase,

${D_c}^{[i,j]}(t, \boldsymbol{S_k})$ is the delay for a lane group with coordinated phase,

$[i,j]$ denotes this is phase group j, at Int. i, and,

$\emptyset_{nc}, \emptyset_c$ are the sets of lane groups with non-coordinated and coordinated phases, respectively.

After optimal timing plans with minimum delays are selected, TOD schedules can be determined correspondingly. This is expressed in Eq. (5. 2).

$$\boldsymbol{S}^*(t) = \text{argmin}_{\boldsymbol{S_k}}\{D(t, \boldsymbol{S_k})\} \quad (5.2)$$

5.2.1 Delay at Non-coordinated Phases

For non-coordinated phases, HCM delay formula is used (TRB, 2000), similar to Park et al. (2004). The calculation is expressed by Eq. (5.3). In the formula, the first term, d_1, estimates uniform control delay, and the second term, d_2, estimates overflow delay. For the sake of brevity, subscript [i, j] is dropped in the right hand side of the formula.

$$D_{nc}^{[i,j]}(t,\boldsymbol{S}) = d_1 + d_2 = v\left\{\frac{0.5C\left(1-\frac{g}{C}\right)^2}{1-\left[\min(1,X)\times\frac{g}{C}\right]} + 900T\left[(X-1)+\sqrt{(X-1)^2+\frac{8klX}{cT}}\right]\right\} \qquad (5.3)$$

Where:

C is the cycle length (s),

g is the effective green time (s),

T is duration of analysis period (h),

k is the incremental delay factor depending on controller setting,

l is the upstream filtering and metering adjustment factor,

v is the lane group volume (veh/hour),

c is the lane group capacity (veh/h), and,

X is volume to capacity (v/c) ratio $= \frac{v}{cg/C}$.

5.2.2 Delay at Coordinated Phases

Eq (5.3) is only suitable to estimate delay with uniform arrivals. Due to coordination impact, the arrivals at the coordinated phases generally cannot be assumed as uniform arrivals. Instead of using Eq (5.3) directly, we calculate the first term of Eq (5.3) at coordinated phases based on a simplified arrival and departure process between two intersections. Here, we assume that main street departure is uniform during green of coordinated phases, and departure from side street is uniform during red. Hence, delay can be calculated numerically, based on the diagram shown in **Figure 5.1**. Note that, this is similar to Hu & Liu (2013). The second term of Eq (5.3) for calculation of overflow delay, remains the same.

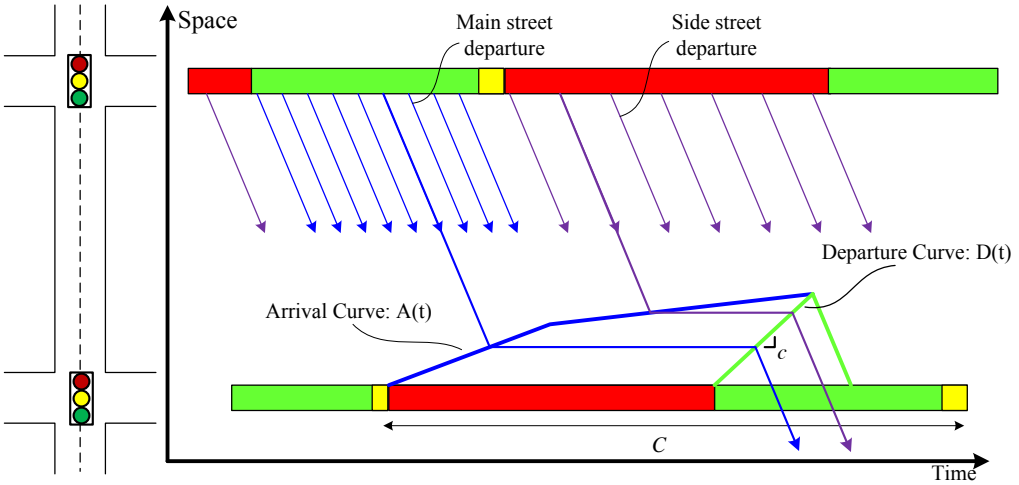

Figure 5.1 Illustration of delay calculation at coordinated phases

Based on the **Figure 5.1**, delay can be calculated as the accumulative difference between arrival traffic and departure traffic. This is expressed in Eq. (5.4).

$$d_1 = \Delta T \sum_{i=1}^{C} \{A(i) - min[A(i), D(i)]\}$$
$$= \Delta T \left\{ \sum_{i=1}^{\lfloor r/\Delta T \rfloor} A(i) + \sum_{i=\lfloor r/\Delta T \rfloor + 1}^{\lfloor C/\Delta T \rfloor} max\{[A(i) - c \times (i - r)], 0\} \right\} \quad (5.4)$$

Where:

ΔT is the time interval to discretize a cycle,

$A(i)$ is the accumulative number of vehicle arrivals,

$D(i)$ is the accumulative number of vehicle departure, and,

r is the effective red time, equals to $C - g$.

Based on upstream volume and signal status, the flow rate $a(k)$ can be calculated as:

$$a(k) = \begin{cases} \frac{q_{u,s}}{C - G_u}, & if\ upstream\ signal\ is\ red\ at\ time\ k \\ \frac{q_{u,m}}{G_u}, & O.W. \end{cases} \quad (5.5)$$

Where:

$a(k)$ is the arrival flow rate at k th interval within cycle,

$q_{u,s}$ is the volume from the site street at upstream intersection,

$q_{u,m}$ is the volume from the main street at upstream intersection, and,

G_u is the green length of coordinated phase at upstream intersection.

Then, the accumulative vehicle arrivals $A(i)$ can be calculated by simply summing up flow rate $a(k)$ as:

$$A(i) = \sum_{k=1}^{i} a(k) \quad (5.6)$$

5.2.3 Estimating Duration Length for Actuated Signals

Clearly, from previous equations i.e. Eq. (5.3) and (5.5), green duration plays an important role in delay calculation. For fixed time signal control, green time is simply a constant that is unaffected by traffic demand. For actuated traffic signals, however, green time varies significantly with different traffic demands. To estimate green time for actuated signals, researches have been done before by calculating gap out and max out probability with random headways (Lin 1982a, 1982b; Akcelik, 1994). Here, we propose a simplified procedure to estimate green time for actuated signals. The main assumption is that the green time is a piecewise linear function depending on arrival volume and pedestrian calls within a cycle, bounded by minimum green and maximum green time. The function is illustrated in **Figure 5.2**. Depending on whether there are any vehicle calls, two cases are considered, as follows:

Case A) If no vehicle is at presence, the signal phase will be either skipped or maintaining pedestrian green plus clearance time if there are any pedestrian calls.

$$f_g(x, Ip) = I_p g_p, \quad if\ x = 0 \tag{5.7A}$$

Where:

x is cycle volume,

I_p is indicator of pedestrian call with 1 means calls and 0 means no call,

$f_g(x, Ip)$ is the duration of green time within a cycle, and,

g_p is the pedestrian green plus clearance time.

Case B) If there are vehicle calls at presence, green time will linearly dependent with vehicle arrivals, constrained by a minimum and maximum green. In case if there are pedestrian calls, corresponding green time must not be smaller than pedestrian green plus clearance time.

$$f_g(x, Ip) = \max\{\min\{\max(c_1 + c_2 x, g_{min}), g_{max}\}, g_p I_p\}, \quad if\ x > 0; \tag{5.7B}$$

Where:

c_1, c_2 are model coefficients,

g_{min} is minimum green, and,

g_{max} is maximum green.

Overall, the function can be expressed as:

$$f_g(x, Ip) = \begin{cases} g_p I_p, & if\ x = 0 \\ \max\{\min\{\max(c_1 + c_2 x, g_{min}), g_{max}\}, g_p I_p\}, & if\ x > 0 \end{cases} \tag{5.8}$$

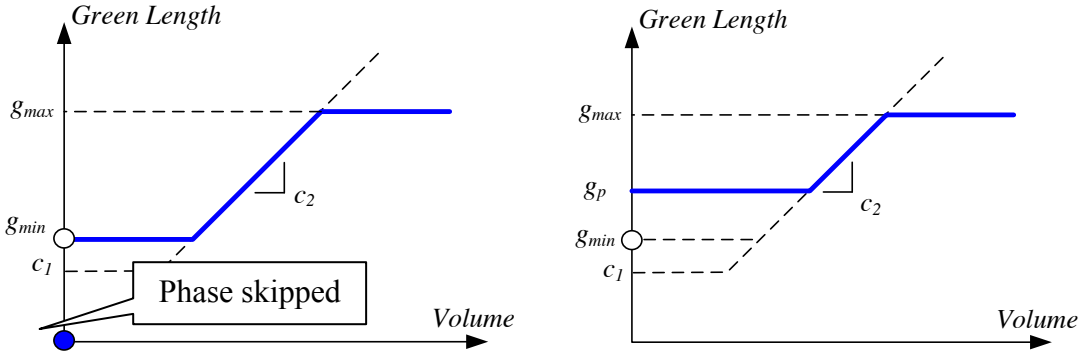

Figure 5.2 Green duration depending on cycle volume without pedestrian calls (left) and with pedestrian calls (right)

Then, Eq. (5.8) is used to calculate average green time over relatively long intervals for further delay calculation. Here, 15 minutes evaluation interval is used, which is the default value from HCM. The average green conditioning on volume, $\bar{g}(x)$, can be calculated as:

$$\bar{g}(x) = E\left[f_g(x, I_p)|v, p_p\right] = \sum_{x, I_p} f_g(x, I_p) \Pr(x, I_p|v, p_p) \tag{5.9}$$

Where:

$\Pr(x, I_p)$ is probability for (x, I_p).

v is average cycle volume during a 15-minute evaluation period, and,

p_p is probability of pedestrian calls during a cycle.

Assuming Poisson distribution for volume x, and Bernoulli distribution for occurrence of pedestrian calls, I_p, with additional assumption that x, I_p are independent, we will have:

$$\Pr(x, I_p | v, p_p) = \frac{v^x e^{-x}}{x!} p_p^{I_p} (1 - p_p)^{1-I_p} \quad (5.10)$$

Unfortunately, an explicit form for Eq. (5.10) is difficult to obtain. Instead, numerical calculation is used, which eventually leads to a table relating average green to volume and probability of pedestrian calls.

To better illustrate the estimation model described above, a numerical example is demonstrated here. Considering hypothetic parameters as, $p_p = 10\%$, $c_1 = 4\ s$, $c_2 = 3\ s$, $g_{min} = 10\ s$, $g_{max} = 25\ s$, $g_p = 30s$, $C = 160\ s$, then in such setting, green time over a cycle without pedestrian call, $f_g(x, 0)$, is shown in sub-figure (A) in **Figure 5.3**. The average green time is shown in sub-figure (B) in **Figure 5.3**. The curves in sub-figure (B) is similar with but smoother than sub-figure (A), due to that $E[f_g(x, I_p)|v, p_p]$ is simply a transformation of $f_g(x, I_p)$. The v1 and v2 in the figure refer to traffic volumes that minimum and maximum green can serve correspondingly.

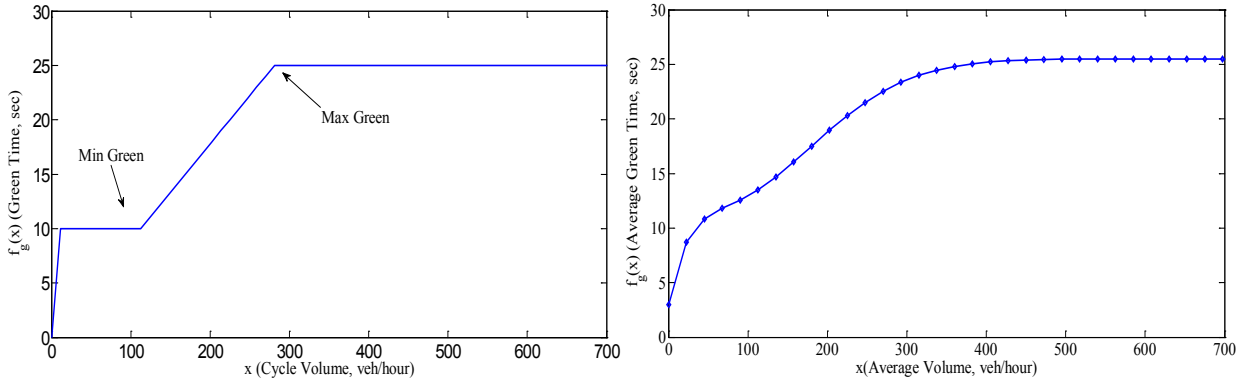

Figure 5.3 Cycle green duration depending on cycle volume (A) and average green duration depending on average volume (B)

5.3 Case Study

To test the proposed methodology, high-resolution event-based traffic data were collected from 7 intersections on Trunk Highway (TH) 13, via SMART-Signal System (Liu et al., 2008; Liu et al., 2013). The data was first used to verify the green time estimation procedure described in this chapter. Then, a simulation experiment was conducted to fine-tune the TOD transitions, based on a commercial traffic simulator VISSIM. The layout of interested segment is shown in **Figure**

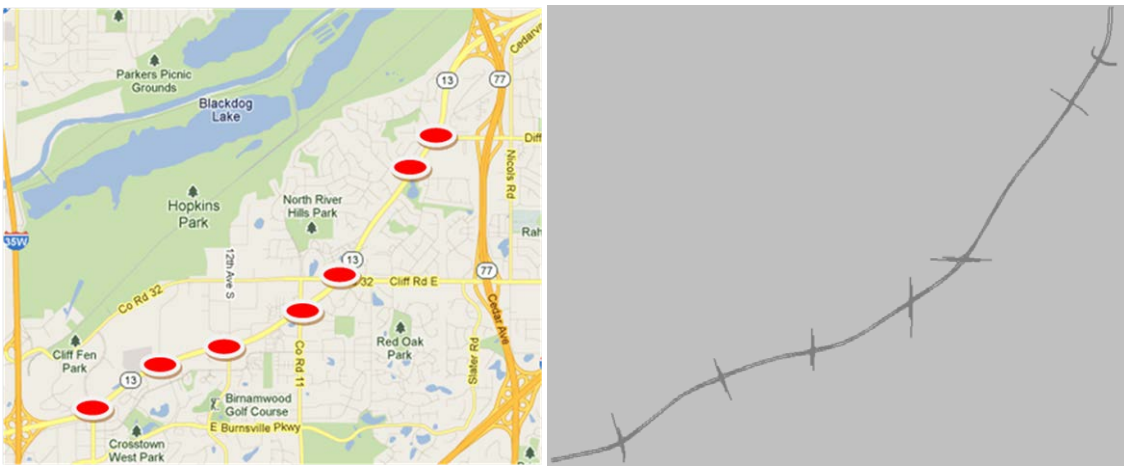

Figure 5.4 Layout of interested segment from Google Map (Left) and layout of simulated road network in VISSUM (Right)

5.3.1 Estimating green time

The selected intersections run coordinated-actuated traffic signals. The through phases at main street, Highway 13, are designated as coordinated phases with site street phases in actuated mode. For left turn phases at main street, there are two configurations: if left turn phase is leading through phase, the left turn will be in actuated mode; if left turn phase is lagging through phases, it will be running essentially as fixed time control, to guarantee a fixed determination point (or reference point) for coordinated phases. A typical configuration, regarding whether a phase is coordinated, actuated or fixed, is illustrated by the ring-and-barrier diagram in **Figure 5.5**. In this case, phases 2 and 6 for EB movement and WB movement are coordinated. Phases 5, 4 and 8 are actuated. Due to fixed force off points associated with phase 2 and phase 1, phase 1 will be fixed if there are any vehicle calls. Otherwise, phase 1 will be skipped.

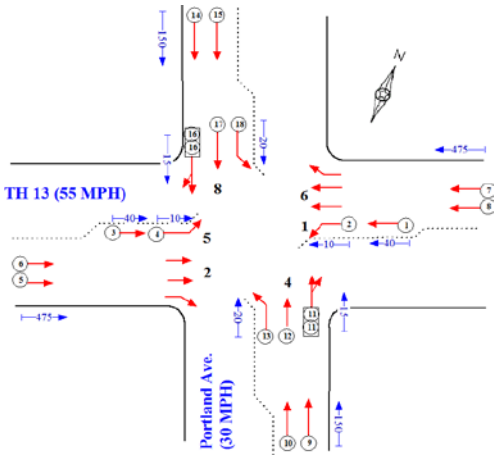

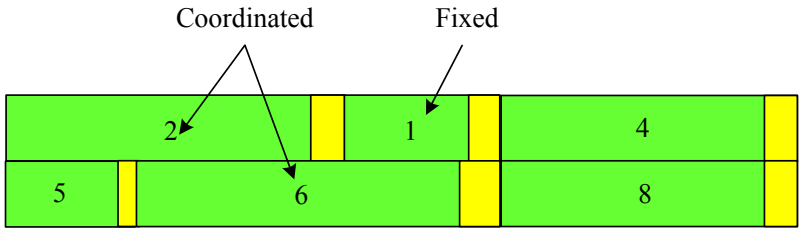

(Phase 3,4,5,7,8 are actuated)

Figure 5.5 Intersection layout and Ring-and-Barrier Diagram at Int. TH13 & Portland Ave.

Utilizing volume data collected from 10/21/2013 to 10/24/2013, Monday to Thursday, green time depending on volume for non-coordinated phases are estimated, using 4 sec for c_1 and 3 sec for c_2. These two values of the model constants have been manually tuned so that the estimation yields a reasonable match with observed value. The results are plotted in **Figure 5.6**. Note that in sub-figure (A), as phase 1 is skipped in some cycles, the average green time over 15 minute interval could be less than the fixed value which is 14.5 sec, as indicated by letter A. Clear biased estimations are shown for phase 4, indicated by letter B. This is due to that phase 8 is more congested than phase 4, and hence is the critical phase in the two ring. Hence, the green time of phase 4 and 8 is mainly determined by demand at phase 8 rather than phase 4. At phase 5 and 8, the estimated curves match generally well with observed data, while better estimation is found at phase 5. This is due to that there is only one lane at phase 5, while multiple detectors and lanes at phase 8. Hence, the extension mechanism at phase 8 is more complicated, and cannot be fully capture by the simple model proposed here.

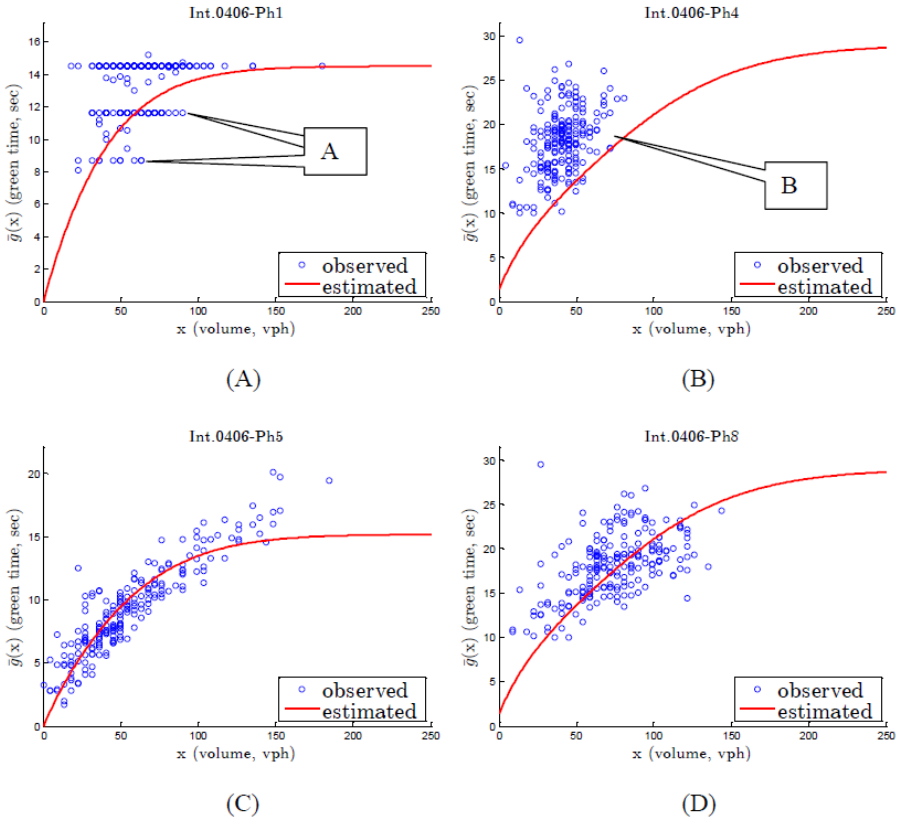

Figure 5.6 Estimated green time VS observed green time depending on 15 minutes volume (A) phase 1, (B) phase 4, (C) phase 5 and (D) phase 8.

After duration of non-coordinated phases are determined, the duration of coordinated phases can be calculated, since the cycle length are fixed for coordinated signals. The comparison of estimated green versus the observed green for the coordinated phases is shown in **Figure 5.7**. As can be seen from the figure, the estimated values match the observed values relatively well for both of the coordinated phases.

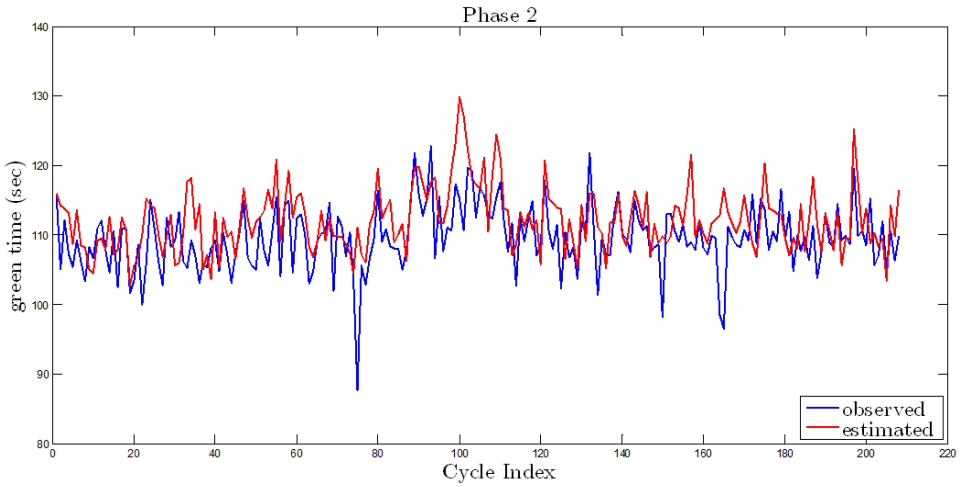

(A)

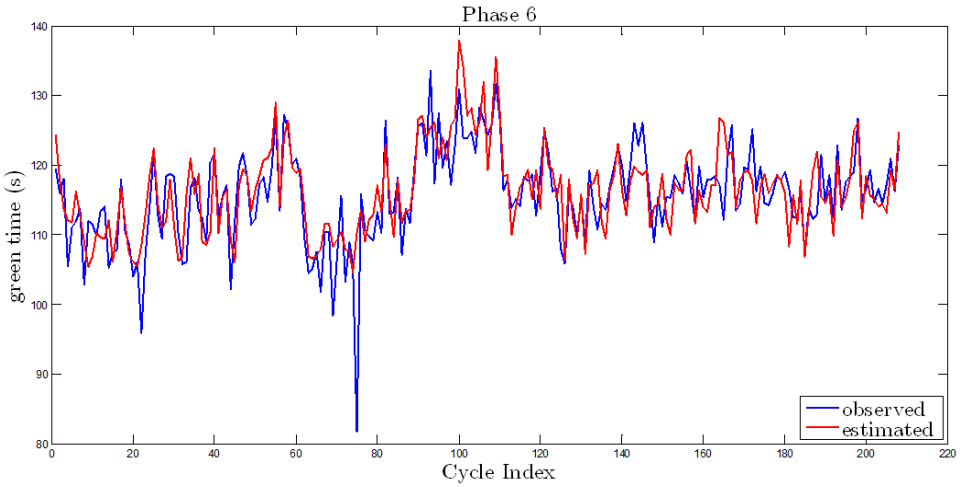

(B)

Figure 5.7 Estimated green time VS observed green time for coordinated phases

5.3.2 Fine-tuning TOD based on delay

In the next, data collected on 10/28/2013, Monday, was highlighted to demonstrate the procedure for TOD transitions fine-tuning. The 15-min interval average volume on the main street was shown in **Figure 5.8**. Clearly, AM peak and PM peak periods can be identified based on the volume patterns. In the AM peak period, EB volumes is heavier than the WB volumes, while reversed volume condition exists during PM peak period. In total, there are 8 timing plans

in operation for weekdays. Periods with different timing plans are separated by black lines, indicating TOD transition points. For the purpose of illustration, here, we only focus on fine-tune TOD transition points between PM off-peak timing plan, and PM-peak timing plan, as indicated by the dash line in **Figure 5.8**.

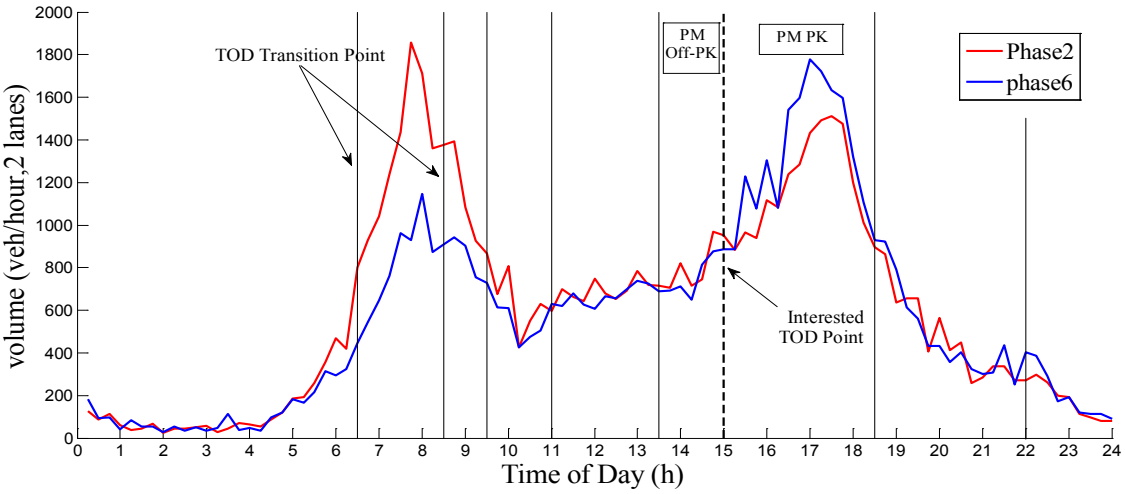

Figure 5.8 Main-street volume over time of day

PM off-peak plan runs from 1:30 PM to 3:00 PM, and PM peak plan runs from 3:00 PM to 6:30 PM. Hence, the transition point is at 3:00 PM. For PM off-peak plan, cycle time is set as 130 sec, while 160 sec cycle time is used for PM peak plan. The green splits are comparable between the two plans at most of phases, except that slightly more green time is assigned to the main street phases in PM peak plan.

Based on the procedure described in section 5.3, the total delays over time for both of the plans are plotted in **Figure 5.9**. The blue line is delay assuming PM-peak plan is running all day, and red line is for PM-off-peak plan. As indicated in the figure, off-peak plan performs better throughout the day than the PM-peak plan. This is unexpected at first, but understandable when considering the longer cycle length for the PM-peak plan, as cycle length plays a critical role in delay calculation. In the original design for this case, cycle length is mainly determined based on traffic conditions at coordinated phases, which are prioritized than the non-coordinated phases. Nevertheless, based on **Figure 5.9**, the optimal choice regarding total delay would be to run off-peak plan through 1:30 PM to 6:30 PM, instead of running two plans during this period.

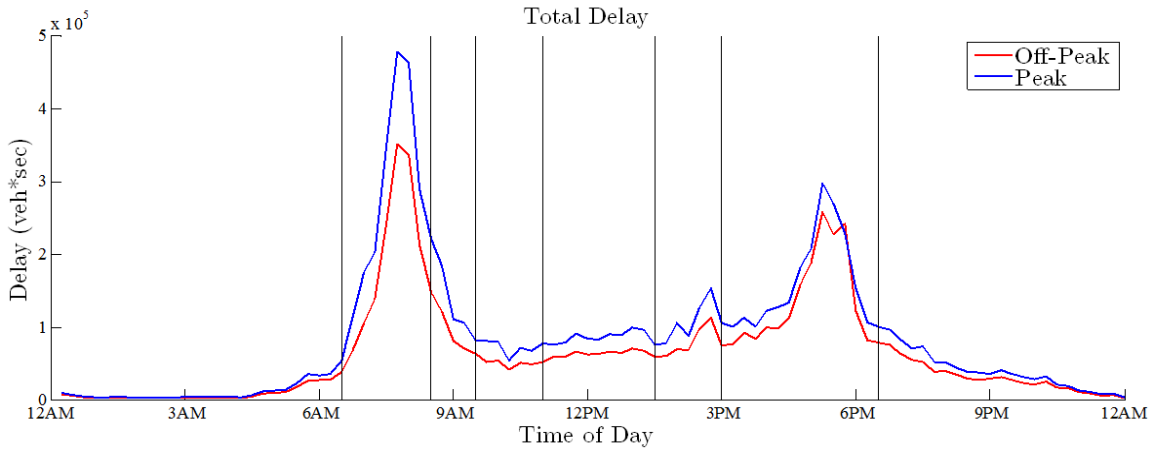

Figure 5.9 Total delays over TOD for the two timing plans

To further investigate the performance of these two plans, delays at the main street were also calculated and plotted in **Figure 5.10**. The PM peak plan performs better than Off-peak plan from 4:30 PM to 6:00 PM, as indicated in the figure. Obviously, if only considering delay at the main street, the optimal choice would be to run peak hour plan from 4:30 PM to 6:00 PM.

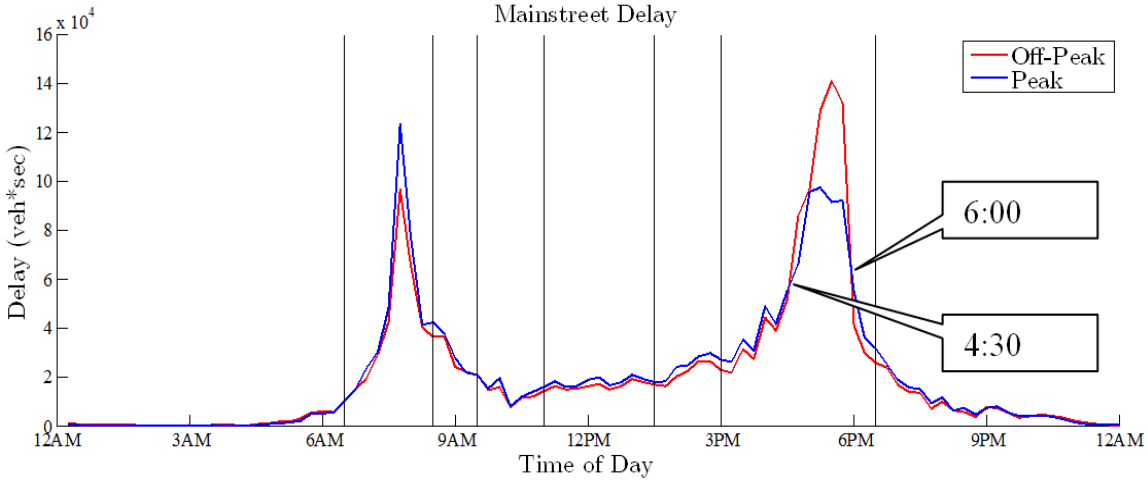

Figure 5.10 Delay at the main street for the two timing plans

Considering priority at the main street imposed by the agency, a proper decision, while conservative, will be to set transition point at 4:30 PM between the two plans, instead of 3:00 PM. Hence, in the modified schedule, the Off-peak plan runs from 1:30 PM to 4:30 PM, and peak plan runs from 4:30 to 6:30 PM. Note that, only one point, 3:00 PM, is being fine-tuned even though two transition points are identified, 4:30 PM and 6:00 PM.

The modified schedule and original schedule were then tested by VISSIM to verify the performance. In total, 5 simulation runs were conducted, and network performance regarding delays and vehicle stops are averaged and listed in **Table 5.1**. As indicated in the table, with the modified schedule, average delay decreased by 5%, average vehicle stops decreased by 4%, comparing to the original schedule. Delays at the main street decreased by 2%, while stops decreased by 1%. The improvement verifies that the modified schedule improves signal performance over the original schedule. The effectiveness of the model was thus validated.

Table 5.1. Performance comparison between original and modified schedules

	Original Schedule	Modified Schedule	Relative Change
Delay per veh [s]	78.94	74.99	-5%
# of stops per veh	1.83	1.76	-4%
Delay per veh, main street [s]	23.76	23.39	-2%
# of stops per veh, main street	0.54	0.53	-1%

5.4 Conclusions

In this chapter, we propose an easy-to-use procedure for TOD fine-tuning for signalized arterial. HCM equations are adopted and modified for delay calculation. We propose a simple but effective model to estimate phase duration length for the actuated traffic signals. Using high resolution event based traffic data from SMART-Signal system, the green estimation algorithm is validated, and TOD fine-tuning procedure is demonstrated. The proposed modification is then verified using VISSIM simulation, showing slight improvements over unmodified schedule. The proposed procedure can be easily implemented using detector and signal data collected from coordinated actuated traffic signals. The objective is to assist the practitioners to fine-tune TOD transitions during signal retiming process. It can also be utilized to fine tune the TOD transitions periodically, thus to help make TOD schedules more responsive to traffic pattern changes.

CHAPTER 6
CONCLUDING REMARKS AND FUTURE RESEARCHES

6.1 Concluding Remarks

Due to the increasing needs to improve traffic management, performance measure for signalized networks has become an emerging focus in the U.S (Liu et al., 2008). However, despite the availability of detectors, few agencies have archived or analyzed detector and signal data at signalized intersections to help signal operations. In this study, by using data collected from existing traffic signal systems, a systematic tool is successfully developed for performance visualization and fine-tuning of the arterial traffic signal system. The objective of this study is to provide convenient tools for the agencies to automate at least partially the signal retiming process, to reduce costs associated with signal retiming, and help agencies maintain efficient signal operations.

In detail, this study:

- An easy to implement framework was proposed for cycle length, offsets wheel and split fine-tuning. Simplified algorithms for the three parameters were described, that can be used for a preliminary and quick fine-tuning.
- Regarding more advanced fine-tuning for the evaluation and fine-tuning of offsets, we proposed a practical procedure to construct the TS-Diagram to visualize progression qualities of signalized arterials. Based on the data collected automatically, the TS-Diagram can be constructed periodically without significant labor cost. The field examples were demonstrated for the proposed TS-Diagrams, and reasonable agreements were found for validation using detector data and vehicle trajectories. A field experiment was also carried out to illustrate the application of TS-Diagram for adjusting offsets and lead-lag sequence. By intuitively evaluating the TS-Diagram, changes were recommended and a 4% reduction of total delays was achieved.
- For the evaluation and fine-tuning of green splits, an adjusted MOE, the UGT, was proposed, extended from queue service time. The ring-and-barrier diagram was adopted to tabulate the information for performance visualization and evaluation. Field examples were also illustrated to demonstrate implementation potential.
- For fine-tuning TOD transition points, a simple algorithm was developed for delay calculation on coordinated arterials. In the present algorithm, signal coordination and actuation are explicitly considered using field collected data. The algorithm was then verified by a simulation study.

There are two potential applications of the signal operations in current practice that the proposed algorithms are intended to help:

(1) They can be employed to validate traffic patterns and fine-tune signal parameters during signal retiming process, thus reducing associated labor costs.

(2) It can be used to evaluate the signal performance periodically, and help engineers to identify adjustment opportunities for improvements, thus maintaining efficient signal operations over time.

6.2 Limitations and Future Research

Limitations of the proposed approaches are discussed in this section. For the TS-Diagram, because traffic patterns at oversaturated intersections are not represented accurately, applications of the proposed approach to oversaturated cases should be avoided. In addition, the proposed approach tends to underestimate queues and delays due to the mechanism that only data on the subject link is considered. In cases with long queues, it may be necessary to consider the upstream intersection jointly to better evaluate traffic conditions. For TOD fine-tuning, the transition costs are not taken into account by the proposed procedures.

Our next step is to try to improve the accuracy of the TS-Diagram by incorporating data from adjacent intersections and incorporate the transition costs into to the TOD fine-tuning algorithm. Another focus will be to extending the application scope from signalized corridors to an area-wide signalized network, such as a grid network in a central business district (CBD), for a more complete evaluation of traffic signal systems.

REFERENCES

1. Abbas, M., Bullock, D. M., & Head, L. (2001). "Real-Time Offset Transitioning Algorithm for Coordinating Traffic Signals." *Transportation Research Record* 1748, 26–39.
2. Abbas, M., & Sharma, A. (2005). "Optimization of time of day plan Scheduling using a multi-objective evolutionary algorithm." Paper presented at the *84th Annual TRB Meeting*, Washington D.C
3. Akcelik, R. (1994). "Estimation of green times and cycle time for vehicle-actuated signals." *Transportation Research Record*, (1457).
4. Ahmed, A. & Brain, J (2008). *An Intersection Traffic Data Collection Device Utilizing Logging Capabilities of Traffic Controllers and Current Traffic Sensors*. NIATT Report Number N08-13.
5. Balke, K., & Herrick, C. (2004). *Potential Measures of Assessing Signal Timing Performance Using Existing Technologies*. TTI.
6. Balke, K., Charara, H. & Parker, R. (2005). *Development of a Traffic Signal Performance Measurement System* (TSPMS). TTI Report No. 0-4422-2.
7. Bullock, D., & Catarella, A. (1998). "A Real-Time Simulation Environment for Evaluating Traffic Signal Systems". Paper presented at the *77th Annual TRB Meeting*, Washington D.C.
8. Day, C. M., Bullock, D. M., & Sturtevant, J.R. (2009). "Cycle-Length Performance Measures: Revisiting and Extending Fundamentals". *Transportation Research Record*, 2128: 48-57.
9. Day, C. M., Sturdevant, J.R., & Bullock, D.M. (2010a)." Outcome-Oriented Performance Measures for Management of Signalized Arterial Capacity." *Transportation Research Record*, 2192: 24–36.
10. Day, C. M., Haseman,R., Premachandra, H., Brennan, Jr., T.M., Wasson, J. S., Sturdevant, J. R. & Bullock, D. M. (2010b). "Evaluation of Arterial Signal Coordination". *Transportation Research Record*, 2192: 37–49.
11. Day, C. M., & Bullock, D. M. (2011). Computational Efficiency of Alternative Algorithms for Arterial Offset Optimization. Transportation Research Record, 2259:37-47.
12. Denney, R.W., Curtis, E., & Head, L (2009) "Long Green Times and Cycles at Congested Traffic Signals," *Transportation Research Record* 2128, 1-10.
13. Gartner, N., & Little, J. D. C. (1975). "Generalized Combination Method for Area Traffic

Control". *Transportation Research Record*, 531: 58–69.

14. Gartner, N. H., Assmann, S. F., Lasaga, F. & Hou, D. L. (1990). "MULTIBAND: A Variable-Bandwidth Arterial Progression Scheme." *Transportation Research Record*, 1287: 212–222.
15. Gettman, D., Shelby, S. G., Head, L., Bullock, D. M., & Soyke, N. (2007). "Data-driven algorithms for real-time adaptive tuning of offsets in coordinated traffic signal systems."*Transportation Research Record*, 2035(1), 1-9.
16. Gordon, R.L. (2010). *Traffic Signal Retiming Practices in the United States*, National Cooperative Highway Research Program (NCHRP).
17. Gordon, R.L. & Braud, C. (2009). *Traffic Signal Operations and Maintenance Staffing Guidelines*, Report FHWA-HOP- 09-006, Federal Highway Administration, Washington, D.C.
18. Gordon, R.L. & Tighe, W. (2005). *Traffic Control Systems Handbook*. Federal Highway Administration.
19. Henry, D. (2005). *Signal Timing on a Shoestring*, Sabra Wang & Associates, Inc., Report FHWA-HOP-07-006, Federal Highway Administration, Washington, D.C..
20. Hu, H., & Liu, H. X. (2013). "Arterial offset optimization using archived high-resolution traffic signal data." *Transportation Research Part C: Emerging Technologies*, 37, 131-144.
21. Husch, D., & Albeck, J. (2006). *Synchro Studio 7 user guide*. Trafficware Ltd., Sugar Land, TX.
22. Koonce, P., Rodegerdts, L., Lee, K., Quayle, S., Beaird, S., Braud, C., Bonneson, J., Tarnoff, P. & Urbanik., T. (2008). *Traffic Signal Timing Manual*. FHWA. Report No. FHWA-HOP-08-024.
23. Khosla, K. and Williams, J. C., (2006). "Saturation Flow at Signalized Intersections during Longer Green Time." *the 85th Annual Meeting of the TRB*, Washington D. C.
24. Lawrence, A. K., Mills, M. K. & Gibson, D. R. P. (2006). Traffic Detector Handbook: Third Edition—Volume I. FHWA.
25. Little, J. D. C., Kelson, M. D. & Gartner, N. H. (1981). "MAXBAND: A Program for Setting Signals on Arteries and Triangular Networks*," Transportation Research Record*, 795:40–46.
26. Liu, H. X., Ma, W., Hu, H., Wu, X., & Yu, G. (2008). "SMART-SIGNAL: Systematic Monitoring of Arterial Road Traffic Signals." In *Intelligent Transportation Systems, 2008*.

ITSC 2008. 11th International IEEE Conference on (pp. 1061-1066). IEEE.

27. Liu, H. & Ma, W. (2009). "A virtual vehicle probe model for time-dependent travel time estimation on signalized arterials". *Transportation Research Part C*, 17 (1): 11-26.
28. Liu, H., Wu, X., Ma, W. & Hu, H. (2009). *Real-time queue length estimation for congested signalized intersections*. Transportation Research Part C, 17 (4): 412–427.
29. Liu, H. X., Zheng, J., Hu, H. & Sun, J. (2013). *Research Implementation of the SMART SIGNAL System on Trunk Highway (TH) 13*. MnDOT Research Report, MN/RC2013-06. Accessible online: http://ntl.bts.gov/lib/47000/47100/47104/MnDOT2013-06_1_.pdf. Accessed on March 15, 2013.
30. Lin, F.B. (1982a). "Estimation of Average Phase Durations for Full-Actuated Signals." In *Transportation Research Record 881*. pp. 65–72.
31. Lin, F. B. (1982b). "Predictive Models of Traffic-Actuated Cycle Splits". *Transportation Research*, Vol. 16B, No. 5, pp. 361–372.
32. Morgan, J.T. & Little, J.D.C. (1964). "Synchronizing Traffic Signals for Maximal Bandwidth." *Operations Research*, Vol. 12, pp. 896-912.
33. National Electrical Manufacturers Association. (2003). "NEMA Standards Publication TS 2". National Electrical Manufacturers Association. Rosslyn, VA.
34. Newell, G. F. (2002). "A simplified car-following theory: a lower order model." *Transportation Research Part B*, 36(3), 195-205.
35. Park, B. B., Santra, P., Yun, I., & Lee, D. H. (2004). "Optimization of time-of-day breakpoints for better traffic signal control". *Transportation Research Record*, 1867(1), 217-223.
36. Park, B. B., & Lee, J. (2008). "A procedure for determining time-of-day break points for coordinated actuated traffic signal systems." *KSCE Journal of Civil Engineering*, 12(1), 37-44.
37. Ratrout, N. T. (2010). "Subtractive clustering-based k-means technique for determining optimum time-of-day breakpoints". *Journal of Computing in Civil Engineering*, 25(5), 380-387.
38. Robertson, D. I., & Bretherton, R. D. (1991). "Optimizing networks of traffic signals in real time-the SCOOT method." *IEEE Transactions on Vehicular Technology*, 40(1), 11-15.
39. Skabardonis, A. (1996). "Determination of timings in signal systems with traffic-actuated

controllers." Transportation Research Record, 1554, 18–26.

40. Smaglik E.J., Sharma, A., Bullock, D.M., Sturdevant, J.R. & Duncan, G. (2007). "Event-Based Data Collection for Generating Actuated Controller Performance Measures". *Transportation Research Record*, 2035, 97–106.
41. Smaglik, E. J., Bullock, D. M., Gettman, D., Day, C. M. & Premachandra, H. (2011). "Comparison of Alternative Real-Time Performance Measures for Measuring Signal Phase Utilization and Identifying Oversaturation." *Transportation Research Record* 2259: 123–131.
42. Smith, B.L., Scherer, W.T., Hauser, T.A., & Park, B.B. (2002). "Data-Driven Methodology for Signal Timing Plan Development: A Computational Approach." *Computer-Aided Civil and Infrastructure Engineering*, 17, 387-395.
43. Sunkari, S. R., Charara, H. A. & Songchitruksa, P. (2011). *A Portable Toolbox to Monitor and Evaluate Signal Operations*. TTI Report No. 0-6177-1.
44. TRB. (2000). Highway Capacity Manual. National Research Council, Washington, D.C.
45. Wallace, C. E., Courage, K. G., Hadi, M. A., & Gan, A. C. (1998). TRANSYT-7F user's guide. Transportation Research Center, University of Florida, Gainesville, Florida.
46. Wang, X., Cottrell, W., & Mu, S. (2005). "Using k-means clustering to identify time-of-day break points for traffic signal timing plans". In *Intelligent Transportation Systems*, 2005. Proceedings. 2005 IEEE (pp. 586-591). IEEE.
47. Webster, F. V. (1958). *Traffic Signal Settings*. TRRL Report 39. U.K. Transport and Road Research Laboratory, London.
48. Wood, K., Palmer, J. P. & Bretherton, R. D. (1994). *Congestion Analysis and Diagnosis*, Transport Research Laboratory, UK (TRL).
49. Wu, X., Liu, H. & Gettman, D. (2010). "Identification of Oversaturated Intersections Using High-Resolution Traffic Signal Data". *Transportation Research Part C*, 18 (4): 626–638.
50. Wu, X. & Liu, H. (2011) "A Shockwave Profile Model for Congested Urban Arterials," Transportation Research Part B, 45(10), 1768-1786.7.
51. Yin, Y., Li, M., & Skabardonis, A. (2007a). "Offline Offset Refiner for Coordinated Actuated Signal Control Systems." Journal of transportation engineering, 133(7), 423-432.
52. Yin, Y. (2008) "Robust optimal traffic signal timing." *Transportation Research Part B* 42, 911-924.
53. Yin, Y., Liu, H., Laval, J.A., Lu, X.Y., Li, M., Pilachowski, J., & Zhang, W., (2007b)

Development of an Integrated Microscopic Traffic Simulation and Signal Timing Optimization Tool. California PATH Research Report, University of California, Berkeley.

54. Zhang, L., & Yin, Y. (2008). "Robust synchronization of actuated signals on arterials." *Transportation Research Record*, 2080(1), 111-119.
55. Zhang, L., Yin, Y., & Lou, Y. (2010). "Robust signal timing for arterials under day-to-day demand variations." *Transportation Research Record*, 2192(1), 156-166.
56. Zheng, J., Liu, H., Misgen, S. & Yu, G. (2013). "Performance Diagnosis Tool for Arterial Traffic Signals." *Transportation Research Record*, 2356(1), 109-116.